Hyperbolic Conservation Laws and Industrial Applications

Michael Junk

FB Mathematik
Universität Kaiserslautern

May 2001

Contents

Preface

This manuscript summarizes lectures given in March 2001 during the summerschool on Hyperbolic Partial Differential Equations which took place at the Technical University of Hamburg–Harburg in Germany.

The aim is to review theoretical aspects of conservation laws based on concrete physical and technical examples. Starting from initial and boundary value problems for scalar equations, the concept of weak solutions and entropy up to the theory of systems of equations are introduced. Examples from various applications in natural sciences and engineering are given, including Euler equations in fluid dynamics, traffic flow problems, acoustics, radiation transfer, crystal growth, and shallow water equations.

1 Transport theorem and balance laws

The starting point of many mathematical models in science and technology are balance considerations of the physical quantities mass, momentum, and energy. As examples we will present the Euler and Navier-Stokes equations, the Saint-Venant equations, and kinetic equations like the Vlasov or Boltzmann equations.

In other cases, one is interested in the number distribution of certain objects (cars in traffic models, individuals in population models, or silver halide crystals in the production of photographic emulsions), and again, balance considerations are the key for setting up a suitable model.

1.1 The flux vector

An important concept in the derivation of balance laws is the *flux vector* $\boldsymbol{q}(t,\boldsymbol{x})$. Let us consider a situation in which mass is transported. This process is completely described by the mass flux $\boldsymbol{q}(t,\boldsymbol{x})$ which provides the amount of mass m that is transported through a surface element ΔS with normal $\boldsymbol{n}$ at a point $\boldsymbol{x}$ during a time interval $[t,t+\Delta t]$

$$m = \boldsymbol{n} \cdot \boldsymbol{q}(t,\boldsymbol{x})\Delta S \Delta t.$$

Note that the flux is maximal for $\boldsymbol{n}$ parallel to $\boldsymbol{q}$ (see Fig. 1.1), $m = 0$ if $\boldsymbol{q}$ is tangential to the surface, and $m < 0$ if the direction of transport is opposite to $\boldsymbol{n}$.

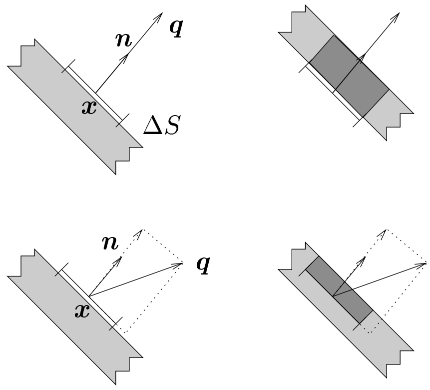

Figure 1.1 Flux through a surface element ΔS with different directions of $\boldsymbol{q}$

Let us now consider a volume A which contains the mass $M_t(A)$ at time t. The increase in mass $\Delta M_t(A) = M_{t+\Delta t}(A) - M_t(A)$ in a small tie interval of length Δt can be due to a flux through ∂A or due to a mass production (or consumption) within A.

Assuming that we know $\boldsymbol{q}$, the total flux through the surface is obtained by integrating contributions $\Delta t(-\boldsymbol{n}) \cdot \boldsymbol{q}\, dS$ along the surface (the negative sign accounts for the fact that $\boldsymbol{n}$ is the outward normal field so that the mass in A increases if $\boldsymbol{q}$ points in direction $-\boldsymbol{n}$ – see Fig. 1.2).

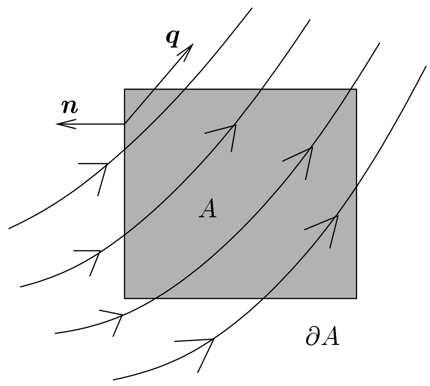

Figure 1.2 Mass increase due to flux through the surface

If $Q(t,\boldsymbol{x})$ is the rate of mass production per volume (which is negative if mass disappears), we obtain the balance relation

$$\Delta M_t(A) = \Delta t \int_{\partial A} (-\boldsymbol{n}) \cdot \boldsymbol{q} \, dS + \Delta t \int_A Q \, d\boldsymbol{x}$$

or in the limit $\Delta t \to 0$

$$\frac{dM_t(A)}{dt} = -\int_{\partial A} \boldsymbol{n} \cdot \boldsymbol{q} \, dS. + \int_A Q \, d\boldsymbol{x}.$$

If the measure $A \mapsto M_t(A)$ has a density u with respect to Lebesgue measure, we obtain the integral form of the balance law

$$\frac{d}{dt} \int_A u \, d\boldsymbol{x} + \int_{\partial A} \boldsymbol{n} \cdot \boldsymbol{q} \, dS - \int_A Q \, d\boldsymbol{x} = 0$$

which holds for all (sufficiently regular) volumes A. If, in addition, $\boldsymbol{q}$ is smooth, we can apply the divergence theorem to transform the surface integral into a volume integral. Dividing by the volume $|A|$ of A and assuming that u is differentiable with respect to t, we find

$$\frac{1}{|A|} \int_A \frac{\partial u}{\partial t} + \mathrm{div} \boldsymbol{q} - Q \, d\boldsymbol{x} = 0.$$

Hence, for a sequence $A_{n,\boldsymbol{x}}$ of volumes which shrinks to a point $\boldsymbol{x}$ for $n \to \infty$, the mean value theorem implies

$$\frac{\partial u}{\partial t} + \mathrm{div} \boldsymbol{q} - Q = 0. \tag{1.1}$$

The balance law (1.1) is called *conservation law*, if $Q \equiv 0$, i.e. if mass is neither produced nor destroyed.

Introducing the space–time variable $\boldsymbol{y} = (t,\boldsymbol{x})$, we can rewrite (1.1) in a simple divergence form

$$\mathrm{div}_{\boldsymbol{y}} \mathcal{A} = Q, \qquad \mathcal{A} = (u,\boldsymbol{q}) \tag{1.2}$$

which will be very useful later.

Up to know, we have assumed that we know both the flux vector $\boldsymbol{q}$ and the source term Q. In a specific application, the modeling therefore consists in deriving expressions for $\boldsymbol{q}$ and Q. This modeling step typically requires a lot of insight into the problem because the structure of $\boldsymbol{q}$ and Q will not be given by general rules. However, if the flux of the balanced quantity is partly caused by a spatial motion, the *transport theorem* helps to specify $\boldsymbol{q}$.

1.2 The transport theorem

We describe a flow in the space $\mathbb{R}^d$ by the flow map $\Pi : \mathbb{R}^+ \times \mathbb{R}^d \to \mathbb{R}^d$ which assigns to a point $\boldsymbol{x} \in \mathbb{R}^d$ its location $\Pi(t,\boldsymbol{x}) = \Pi_t(\boldsymbol{x})$ after following the flow for a time $t \in \mathbb{R}^+$ (see Fig. 1.3).

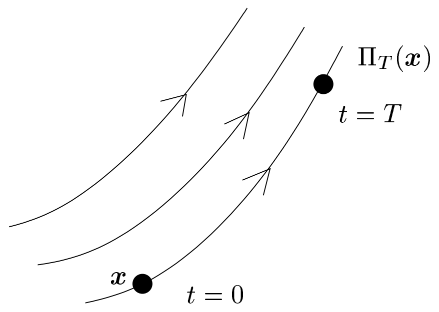

Figure 1.3 Action of the flow map Π

The flow velocity $\boldsymbol{a}$ associated to this movement is given by the partial time derivative of Π

$$\boldsymbol{a}(t,\Pi_t(\boldsymbol{x})) = \frac{\partial \Pi_t(\boldsymbol{x})}{\partial t}.$$

In many practical cases, the modeling step yields an expression for the flow velocity $\boldsymbol{a}$ and $\Pi_t(\boldsymbol{x}) = \boldsymbol{z}(t)$ is then defined as solution of the ordinary differential equation $\dot{\boldsymbol{z}}(t) = \boldsymbol{a}(t,\boldsymbol{z}(t))$, $\boldsymbol{z}(0) = \boldsymbol{x}$.

In analogy to our considerations in the previous section, we want to set up a balance relation but now for volumes $\Pi_t(A)$ which move with the flow. An expression for the rate of change of $M_t(\Pi_t(A))$ is then given by the transport theorem:

Theorem 1 *Let* $\Pi \in C^1(\mathbb{R}^+ \times \mathbb{R}^d)$, *and* $\Pi_t : \mathbb{R}^d \to \mathbb{R}^d$ *be injective with* $\det(\nabla \Pi_t) > 0$ *for every* $t \in \mathbb{R}^+$. *Assume further that*

$$M_t(A) = \int_A u(t,\boldsymbol{x})\, d\boldsymbol{x}$$

is a measure with density $u \in C^1(\mathbb{R}^+ \times \mathbb{R}^d)$ *and that* A *is an open bounded set with a* C^1 *-boundary. Then*

$$\frac{d}{dt} M_t(\Pi_t(A)) = \int_{\Pi_t(A)} \frac{\partial u}{\partial t} + \operatorname{div}(u\boldsymbol{a})\, d\boldsymbol{y} \tag{1.3}$$

where $\boldsymbol{a}(t,\Pi_t(\boldsymbol{x})) = \frac{\partial \Pi_t(\boldsymbol{x})}{\partial t}$ *is the flow velocity.*

Proof: We only present the main idea of the proof and refer to [2] for details. First, we introduce the change of variables $\boldsymbol{y} = \Pi_t(\boldsymbol{x})$ so that

$$M_t(\Pi_t(A)) = \int_A u(t,\Pi_t(\boldsymbol{x})) \det D_t(\boldsymbol{x})\, d\boldsymbol{x}$$

where $D_t(\boldsymbol{x})$ has been introduced as abbreviation for $\nabla\Pi_t(\boldsymbol{x})$. Pulling the time derivative under the integral and observing the definition of the flow velocity, we obtain with product and chain rule

$$\frac{d}{dt}M_t(\Pi_t(A)) = \int_A \left(\frac{\partial u}{\partial t} + \boldsymbol{a}\nabla u\right) \det D_t + u\frac{\partial}{\partial t} \det D_t \, d\boldsymbol{x} \tag{1.4}$$

For every fixed $\boldsymbol{x} \in A$, we now consider $D_t = D_t(\boldsymbol{x})$ as an invertible matrix which smoothly depends on a parameter $t \in \mathbb{R}^+$. Using the definition of the determinant, one can show that in such a case

$$\frac{d}{dt}\det D_t = \operatorname{tr}(\dot{D}_t D_t^{-1}) \det D_t \tag{1.5}$$

where tr denotes the trace of a matrix. Using now the special form of $D_t = \nabla\Pi_t$ it turns out that

$$\operatorname{tr}(\dot{D}_t D_t^{-1}) = \operatorname{div}\boldsymbol{a}. \tag{1.6}$$

The result follows by inserting (1.5) and (1.6) in (1.4) and transforming the variables back with $\boldsymbol{x} = \Pi_t^{-1}(\boldsymbol{y})$. ■

With the expression (1.3) for the rate of change of mass in a transported volume, we now set up a balance equation. If Q describes again the rate of mass production per volume and $\tilde{\boldsymbol{q}}$ is the mass flux *relative to the movement*, then the balance law reads

$$\frac{d}{dt}M_t(\Pi_t(A)) = \int_{\partial\Pi_t(A)} (-\boldsymbol{n}) \cdot \tilde{\boldsymbol{q}} \, dS + \int_{\Pi_t(A)} Q \, d\boldsymbol{x}.$$

Using the transport theorem and letting A shrink to a point, we arrive at the differential form of the balance law

$$\frac{\partial u}{\partial t} + \operatorname{div}(u\boldsymbol{a} + \tilde{\boldsymbol{q}}) = Q. \tag{1.7}$$

In particular, if the quantity u under consideration is conserved $(Q = 0)$ and if there are no mechanisms leading to a flux apart from the flow Π, the conservation law is fully determined by the flow velocity

$$\frac{\partial u}{\partial t} + \operatorname{div}(u\boldsymbol{a}) = 0.$$

In the following sections, we see several examples which are based on these assumptions.

1.3 Continuum hypothesis

Very often, the assumption that $M_t(A)$ has a density $u(t,\boldsymbol{x})$ with respect to Lebesgue measure is violated. To give a concrete example, let us consider a model of a large population with a typical size of $\bar{N} = 10^8$ individuals. We assume that $N_t(A)$ is the number of individuals with age $x \in A \subset \mathbb{R}^+$. Obviously, N_t is a discrete measure. In fact, N_t can be written as sum of Dirac measures

$$N_t = \sum_{i\in\mathbb{N}} \omega_i(t)\delta_{x_i(t)}$$

where $x_i(t)$ is the age of individual i at time t and $\omega_i(t) \in \{0,1\}$ indicates whether the individual is alive $(\omega_i(t) = 1)$, or dead $(\omega_i(t) = 0)$. Since the Dirac measure has no density with respect to the Lebesgue measure, the same holds for N_t and we cannot proceed as in section 1.1 and 1.2. However, taking into account that the total population is quite large, it makes sense to approximate N_t by a continuous measure. To illustrate the idea, we consider the cumulative distribution function $x \mapsto N_t([0,x])$ which is a piecewise constant function with jumps at the points $x_i(t)$ and typical jump height one (see fig. 1.4(a)).

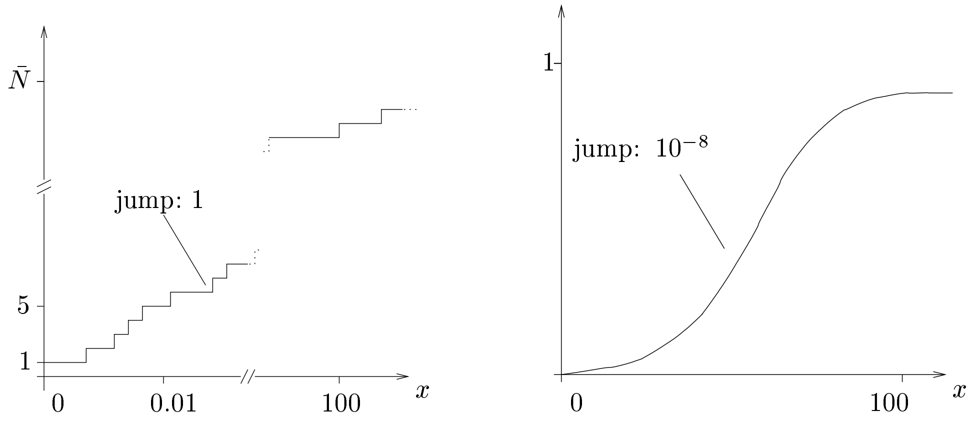

(a) $N_t([0,x])$ (b) $N_t([0,x])/\bar{N}$

Figure 1.4 Unscaled and scaled cumulative age distribution function

The scaled measure $N_t/\bar{N}$, on the other hand, leads to a distribution function with only very small jumps $\bar{N}^{-1}$ and for this function one can postulate the *continuum hypothesis:*

$N_t/\bar{N}$ can be approximated by a measure M_t with (smooth) density $u(t,x)$.

Note that the approximation M_t is a good substitute for $N_t/\bar{N}$ only on sets with relatively large N_t measure. This should be kept in mind when interpreting results derived with u in terms of the underlying population.

1.4 Examples of balance laws

1.4.1 Population model

Applying the continuum hypothesis of the previous section, we introduce

$$M_t(I) = \int_I u(t,x)\,dx$$

as the number of individuals with age $x \in I \subset \mathbb{R}^+$. The only reason for a flow in the "age-space" $\mathbb{R}^+$ is the aging process: an individual with age x at time 0 has age $x + t$ at time t. This gives rise to $\Pi_t(x) = x + t$ and the associated flow speed

$$a(t,x) = \frac{\partial \Pi_t}{\partial t} = 1.$$

The lack of any further flux mechanism implies $\tilde{q} = 0$ in the general balance law (1.7). Since individuals can "disappear" at any age with a certain age dependent death rate $\mu(t,x)$, we obtain the negative production rate $Q(t,x) = -\mu(t,x)u(t,x)$, giving rise to the linear balance law

$$\frac{\partial u}{\partial t} + \frac{\partial u}{\partial x} = -\mu u \tag{1.8}$$

The domain of definition of (1.8) is the (t,x) quarter plane $\Omega = \mathbb{R}^+ \times \mathbb{R}^+$. Natural conditions at the boundaries are $u(0,x) = u^0(x)$ for the condition at $t = 0$ (for example, the situation after a census) and

$$u(t,0) = \int_0^\infty \lambda(t,x)u(t,x)\,dx$$

models the creation of individuals with age $x = 0$ based on an age dependent fertility rate $\lambda(t,x) \geq 0$. This population model is known as Von Foerster model (see [11]).

1.4.2 Traffic model

Applying the continuum hypothesis (heavy traffic), we introduce

$$M_t(I) = \int_I u(t,x)\,dx$$

as the number of vehicles in an interval I of the single lane one-way street $\mathbb{R}$. The only reason for a transport along the road is the movement of the vehicles with velocity $a(t,x)$. In a simple model, we assume that $a(t,x)$ only depends on the local traffic density, i.e. $a(t,x) = V(u(t,x))$ where V is determined from measurements and typically has a shape as indicated in fig. 1.5.

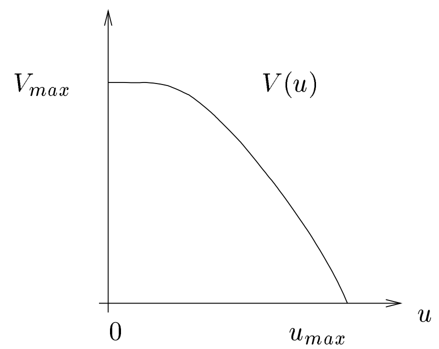

Figure 1.5 Typical dependence of vehicle velocity on traffic density

As additional simplification, we assume that the road has no entrance or exit which yields $Q = 0$. Altogether, we obtain the nonlinear conservation law

$$\frac{\partial u}{\partial t} + \frac{\partial}{\partial x}(uV(u)) = 0 \tag{1.9}$$

with domain of definition $\Omega = \mathbb{R}^+ \times \mathbb{R}$. More complicated models are used to predict traffic situations and to run traffic control systems as shown in fig. 1.6.

Figure 1.6 Traffic control systems are based on mathematical traffic models

While the assumption of a density dependent vehicle velocity is quite intuitive, it can lead to a behavior which is not observed in real traffic flow. The reason is that drivers choose their speed not only based on the local density but also on the rate of change of this density. For example, if the density increases in front, the velocity is already reduced. This behavior gives rise to a more realistic flux

$$q = uV(u) - \alpha \frac{\partial u}{\partial x}, \quad \alpha > 0$$

The corresponding balance equation

$$\frac{\partial u}{\partial t} + \frac{\partial}{\partial x}(uV(u)) = \alpha \frac{\partial^2 u}{\partial x^2} \tag{1.10}$$

is of parabolic type and formally reduces to the hyperbolic model (1.9) for $\alpha \to 0$. Later, when we discuss the concept of weak solutions, the refined parabolic model will be useful to single out the correct (i.e. realistic) weak solution of (1.9).

Before going over to the next example, let us briefly focus on the concept of *linearization*: if the vehicle density only slightly deviates from a constant density $\bar{u}(t,x) = c$, one can approximate the nonlinear model (1.9) by a simpler, linear equation. Formally, the linearization process consists of the following steps: first, the equation is written in terms of a function F depending on u and derivatives of u

$$0 = \frac{\partial u}{\partial t} + q'(u)\frac{\partial u}{\partial x} = F\left(u, \frac{\partial u}{\partial t}, \frac{\partial u}{\partial x}\right)$$

with $F(w_0,w_1,w_2) = w_1 + q'(w_0)w_2$ and $\boldsymbol{w} \in \mathbb{R}^3$. Then, the idea is to replace the nonlinear function F by its linearization

$$F(\boldsymbol{w}) \approx F(\bar{\boldsymbol{w}}) + (\boldsymbol{w} - \bar{\boldsymbol{w}}) \cdot \nabla_{\boldsymbol{w}} F(\bar{\boldsymbol{w}})$$

Substituting $\boldsymbol{w}$ and $\bar{\boldsymbol{w}}$ by

$$\boldsymbol{w} = (u, \frac{\partial u}{\partial t}, \frac{\partial u}{\partial x}), \qquad \bar{\boldsymbol{w}} = (\bar{u}, \frac{\partial \bar{u}}{\partial t}, \frac{\partial \bar{u}}{\partial x})$$

and using the fact that $\bar{u}$ is a specific solution of (1.9) so that $F(\bar{\boldsymbol{w}}) = 0$, we arrive at the linear equation $(\boldsymbol{w} - \bar{\boldsymbol{w}}) \cdot \nabla_{\boldsymbol{w}} F(\bar{\boldsymbol{w}}) = 0$. In the case under consideration, we have $\bar{\boldsymbol{w}} = (c,0,0)$, $\nabla_{\boldsymbol{w}} F(\bar{\boldsymbol{w}}) = (0,1,q'(c))$, and hence

$$\frac{\partial u}{\partial t} + q'(c)\frac{\partial u}{\partial x} = 0 \tag{1.11}$$

as linearization of(1.9).

1.4.3 Kinetic equations

We consider a large number of microscopic particles which behave according to the laws of classical mechanics. In particular, the movement of a single particle in the force field $\boldsymbol{F}(\boldsymbol{x})$ is determined by Newton's law which we write in the form

$$\dot{\boldsymbol{x}} = \boldsymbol{v}, \qquad \dot{\boldsymbol{v}} = \boldsymbol{F}(\boldsymbol{x}).$$

The distribution of the particles in physical space as well as in velocity space is given by the measure

$$M_t(A \times B) = \int_A \int_B f(t,\boldsymbol{x},\boldsymbol{v})\, d\boldsymbol{v}\, d\boldsymbol{x}$$

which describes the mass of particles in $A \subset \mathbb{R}^3$ having velocities in $B \subset \mathbb{R}^3$. Introducing the phase space variable $\boldsymbol{y} = (\boldsymbol{x},\boldsymbol{v})$, the flow velocity which describes the movement of the particles in phase space is given by

$$\boldsymbol{a}(\boldsymbol{y}) = (\boldsymbol{v},\boldsymbol{F}(\boldsymbol{x})), \qquad \boldsymbol{y} = (\boldsymbol{x},\boldsymbol{v}).$$

If there is no additional flux but a source or sink term Q, we obtain the balance law

$$\frac{\partial f}{\partial t} + \operatorname{div}(f\boldsymbol{a}) = Q. \tag{1.12}$$

Since $\operatorname{div}_{\boldsymbol{y}}(f\boldsymbol{a}) = \boldsymbol{a} \cdot \nabla_{\boldsymbol{y}} f + f \operatorname{div}_{\boldsymbol{y}} \boldsymbol{a}$ and $\operatorname{div}_{\boldsymbol{y}} \boldsymbol{a} = \operatorname{div}_{\boldsymbol{x}} \boldsymbol{v} + \operatorname{div}_{\boldsymbol{v}} \boldsymbol{F}(\boldsymbol{x}) = 0$, we can rewrite (1.12) in the form (with $Q = 0$)

$$\frac{\partial f}{\partial t} + \boldsymbol{v} \cdot \nabla_{\boldsymbol{x}} f + \boldsymbol{F}(\boldsymbol{x}) \cdot \nabla_{\boldsymbol{v}} f = 0 \tag{1.13}$$

which is called *Vlasov equation.* Typically, the force field $\boldsymbol{F}$ is generated by the particles themselves (electrical or gravitational field) which gives rise to an additional equation

$$\boldsymbol{F} = -\nabla_{\boldsymbol{x}} \phi, \quad \Delta\phi = \pm \int_{\mathbb{R}^3} f\, d\boldsymbol{v}$$

Important industrial applications of the Vlasov equation arise in the design of systems which use plasma (like plasma engines in space vehicles).

If the particle interactions result from short range forces, it is useful to avoid a detailed description of the force field $\boldsymbol{F}$ and model the interactions with a source term Q. To illustrate this approach, let us consider the case in which two particles with velocities $\boldsymbol{v}'$ and $\boldsymbol{v}'_*$ collide in a point $\boldsymbol{x}$ which means that the velocities instantaneously change into outgoing velocities $\boldsymbol{v}$ and $\boldsymbol{v}_*$ (see fig. 1.7).

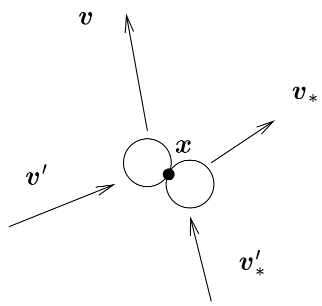

Figure 1.7 Collision of particles

In other words, the particles characterized by $(\boldsymbol{x},\boldsymbol{v}')$ and $(\boldsymbol{x},\boldsymbol{v}'_*)$ disappear, and the pair $(\boldsymbol{x},\boldsymbol{v})$ and $(\boldsymbol{x},\boldsymbol{v}_*)$ suddenly appears. Without going further into details, we mention that the corresponding source term has the form

$$Q(f) = \int_{\mathbb{R}^3}\int_{S^2_+} B(\boldsymbol{v},\boldsymbol{v}_*,\boldsymbol{\xi})(f'f'_* - ff_*)\,d\boldsymbol{\xi}\,d\boldsymbol{v}_* \tag{1.14}$$

where f',f'_*,f_* are equal to f evaluated at the velocities $\boldsymbol{v}',\boldsymbol{v}'_*,\boldsymbol{v}_*$, where $\boldsymbol{v}',\boldsymbol{v}'_*$ depend on $\boldsymbol{v},\boldsymbol{v}_*$ and the vector $\boldsymbol{\xi} \in S^2_+$ (for details see [1]). Using (1.14) together with the flow velocity $\boldsymbol{a}(,\boldsymbol{v}) = (\boldsymbol{v},\boldsymbol{0})$, we obtain the balance law

$$\frac{\partial f}{\partial t} + \boldsymbol{v}\cdot\nabla_{\boldsymbol{x}} f = Q(f)$$

which is the *Boltzmann equation*. Important applications of this equation are rarefied gas flows which appear, for example, during reentry of space vehicles.

1.4.4 Euler equation

The Euler equation is the paradigmatic case of a hyperbolic system of balance laws. Since it describes the flow of gases, it obviously has many technical applications.

The balanced quantities are mass, momentum, and energy with corresponding densities $\rho,\rho\boldsymbol{u},\rho E$. The field $\boldsymbol{u} = \rho\boldsymbol{u}/\rho$ is the flow velocity of the gas. If the flow with velocity $\boldsymbol{u}$ is the only reason for a mass transport (no mass diffusion), and if there are no mass sources, we immediately deduce the balance law for ρ

$$\frac{\partial \rho}{\partial t} + \operatorname{div}(\rho\boldsymbol{u}) = 0 \tag{1.15}$$

The momentum balance is derived with Newton's law which relates the rate of change of momentum of a control volume to forces acting on the volume and its surface. Introducing the stress tensor σ, the force on a surface element dS of the control volume with normal $\boldsymbol{n}$ is $\sigma\boldsymbol{n}\,dS$. In particular, the i th component of the surface force is given by $\boldsymbol{\sigma}_i\cdot\boldsymbol{n}$, where $\boldsymbol{\sigma}_i = (\sigma_{i,1},\sigma_{i,2},\sigma_{i,3})$, so that $-\boldsymbol{\sigma}_i$ acts as additional flux in the balance law for the i th component of $\rho\boldsymbol{u}$. Volume forces which act on every point inside the control volume are incorporated as source term. For example, gravitational forces give rise to the source term $\rho\boldsymbol{g}$ where $\boldsymbol{g}$ is the gravitational acceleration. Altogether, the balance of forces yields

$$\frac{\partial \rho u_i}{\partial t} + \operatorname{div}(\rho u_i\boldsymbol{u}) = \operatorname{div}\boldsymbol{\sigma}_i + \rho g_i, \qquad i = 1,2,3. \tag{1.16}$$

Since the forces acting on the control volume provide or require energy, each force term in the momentum equation leads to a corresponding term in the energy equation. Additional contributions arise from a possible heat flux $\boldsymbol{q}$ and a heat source Q. The energy balance equation has the form

$$\frac{\partial \rho E}{\partial t} + \operatorname{div}(\rho E \boldsymbol{u}) = \operatorname{div}(\sigma \boldsymbol{u}) + \rho \boldsymbol{g} \cdot \boldsymbol{u} - \operatorname{div} \boldsymbol{q} + Q \tag{1.17}$$

Since equations (1.15), (1.16),(1.17) contain more unknowns than equations, the system is not closed and additional closure relations are required. For the Euler equation of an ideal gas, one assumes that the surface forces are only due to pressure $\sigma_{ij} = -p\delta_{ij}$, where pressure is related to temperature $p = \rho RT$, and temperature to energy via $E = |\boldsymbol{u}|^2/2 + RT/(\gamma - 1)$ (R is the universal gas constant and γ is the ratio of heat capacities at constant pressure and constant volume). Heat flux and heat production are typically neglected $\boldsymbol{q} = 0, Q = 0$.

As in the case of the traffic model, the hyperbolic system is only a first model. A more refined approach is given by the Navier-Stokes-Fourier closure, where also friction forces are taken into account and where heat flux is caused by a temperature gradient

$$\sigma_{ij} = -p\delta_{ij} + \mu \left(\frac{\partial u_i}{\partial x_j} + \frac{\partial u_j}{\partial x_i} \right), \qquad \boldsymbol{q} = -\lambda \nabla T.$$

The parameters μ and λ are viscosity and heat conduction coefficients respectively. Equations (1.15), (1.16),(1.17) with these closure relations are called *compressible Navier-Stokes equations.*

Apart from density, pressure, and temperature, another important thermodynamical variable is the entropy ρS

$$\rho S = -\rho \ln \left(\frac{T}{\rho^{\gamma-1}} \right)$$

which is a convex function in terms of the variables $(\rho, \rho\boldsymbol{u}, \rho E)$ of the Euler system. It turns out that for smooth solutions of the Euler system, ρS automatically satisfies the conservation law

$$\frac{\partial \rho S}{\partial t} + \operatorname{div}(\rho S \boldsymbol{u}) = 0 \tag{1.18}$$

which means that entropy is just transported with the velocity $\boldsymbol{u}$. For more general thermodynamical processes (e.g. piecewise smooth solutions of the Euler system with jumps in the variables), one physically expects that the entropy can also decrease (note that we have chosen the negative logarithm in the definition of S), so that a physically more general entropy equation is given by

$$\frac{\partial \rho S}{\partial t} + \operatorname{div}(\rho S \boldsymbol{u}) \leq 0. \tag{1.19}$$

Starting with the Navier-Stokes-Fourier closure, one can, in fact, derive (1.19) by letting μ, λ tend to zero in the equation for the entropy. It turns out that the sign condition in (1.19) is very important to single out the physically correct solution of the Euler system once the solution is not smooth. Another observation is that relations similar to (1.19) are obtained when ρS is replaced by a more general expression of the form

$$\eta_\phi = \rho \phi \left(\frac{T}{\rho^{\gamma-1}} \right)$$

where $\phi : \mathbb{R}^+ \to \mathbb{R}$ satisfies $\phi' \le 0$, $\phi'' \ge 0$. Starting again from the Navier-Stokes-closure, we obtain an evolution equation for the quantity η_ϕ which depends on the unknowns $\rho, \rho\boldsymbol{u}$, an ρE . Letting μ, λ tend to zero in this equation, one ends up with

$$\frac{\partial \eta_\phi}{\partial t} + \mathrm{div}(\eta_\phi \boldsymbol{u}) \le 0 \tag{1.20}$$

which are additional conditions on the physically correct solution of the Euler system (which is the limit system of the Navier-Stokes equation for $\mu \searrow 0$). Although η_ϕ is, strictly speaking, not an entropy, one nevertheless calls η_ϕ a (Lax-) entropy and (1.20) an *entropy condition.* The notion of entropy plays an important role in the theory of hyperbolic conservation laws.

Restricting to the case of smooth solutions of the Euler system and replacing the variable E by the entropy S , equation (1.17) (with the Euler closure and $\boldsymbol{g} = 0$) turns into (1.18) (remember that smooth solutions of the Euler system satisfy (1.18) automatically). Assuming moreover that S is initially constant, equation (1.18) in connection with (1.15) implies that S stays constant for all times. Hence, the Euler system reduces to the mass and momentum equation in this *isentropic case* and $p = \rho RT$ implies that the pressure is a function of density and the constant entropy (via T). More precisely, the isentropic Euler system has the form

$$\begin{aligned}
&\frac{\partial \rho}{\partial t} + \mathrm{div}(\rho \boldsymbol{u}) = 0,\\
&\frac{\partial \rho u_i}{\partial t} + \mathrm{div}(\rho u_i \boldsymbol{u}) + \frac{\partial p}{\partial x_i} = 0, \qquad p(\rho) = C\rho^\gamma.
\end{aligned}$$

Especially in applications where weak acoustic fields are to be calculated, it is reasonable to linearize the isentropic Euler system around the specific solution $\bar\rho(t,\boldsymbol{x}) = \rho_0$, $\bar{\boldsymbol{u}}(t,\boldsymbol{x}) = 0$. The linearization process works as in the case of the traffic flow model and we will explain it only briefly for the mass conservation equation (here we use Einstein's summation convention for repeated indices)

$$0 = \frac{\partial \rho}{\partial t} + u_j \frac{\partial \rho}{\partial x_j} + \rho \frac{\partial u_j}{\partial x_j} = F(\rho, \boldsymbol{u}, \partial_t \rho, \nabla\rho, \mathrm{div}\boldsymbol{u})$$

where $F(w_0, \boldsymbol{w}_1, w_2, \boldsymbol{w}_3, w_4) = w_2 + \boldsymbol{w}_1 \cdot \boldsymbol{w}_3 + w_0 w_4$ with $w_0, w_2, w_4 \in \mathbb{R}$ and $\boldsymbol{w}_1, \boldsymbol{w}_3 \in \mathbb{R}^3$. Replacing f in this equation by its linearization at the point

$$\bar{\boldsymbol{w}} = (\bar\rho, \bar{\boldsymbol{u}}, \partial_t \bar\rho, \nabla\bar\rho, \mathrm{div}\bar{\boldsymbol{u}}) = (\rho_0, 0, 0, 0, 0)$$

we obtain the linear problem

$$\frac{\partial \rho}{\partial t} + \rho_0 \mathrm{div}\boldsymbol{u} = 0 \tag{1.21}$$

Similarly, the momentum conservation equation turns into a linear equation for the velocity

$$\frac{\partial \boldsymbol{u}}{\partial t} + \frac{p'(\rho_0)}{\rho_0} \nabla\rho = 0 \tag{1.22}$$

If the density ρ in (1.21) and (1.22) is replaced by a scaled, linear pressure $p = (p(\rho_0) + p'(\rho_0)\rho)/(p'(\rho_0)\rho_0)$, one obtains the equations of acoustics

$$\frac{\partial p}{\partial t} + \mathrm{div}\boldsymbol{u} = 0, \qquad \frac{\partial \boldsymbol{u}}{\partial t} + p'(\rho_0)\nabla p = 0 \tag{1.23}$$

which will be discussed in detail at the end of section 2.

2 Linear initial and boundary value problems

2.1 The method of characteristics

Recalling the general form of a scalar balance law, we have

$$\frac{\partial u}{\partial t} + \mathrm{div}_{\boldsymbol{x}} \boldsymbol{q} = Q,$$

or with the combined variable $\boldsymbol{y} = (t,\boldsymbol{x})$ and the combined flux $\mathcal{A}(\boldsymbol{y},v) = (v,\boldsymbol{q}(\boldsymbol{y},v))$

$$\mathrm{div}_{\boldsymbol{y}} \mathcal{A}(\boldsymbol{y},u(\boldsymbol{y})) = Q(\boldsymbol{y},u(\boldsymbol{y})). \tag{2.1}$$

Equation (2.1) is linear if $\mathcal{A}$ and Q are (affine-) linear in u, i.e.

$$\mathcal{A}(\boldsymbol{y},v) = \boldsymbol{a}(\boldsymbol{y})v, \qquad Q(\boldsymbol{y},v) = c(\boldsymbol{y}) + d(\boldsymbol{y})v.$$

Denoting $b(\boldsymbol{y}) = -\mathrm{div}_{\boldsymbol{y}} \boldsymbol{a}(\boldsymbol{y}) + d(\boldsymbol{y})$, we obtain

$$\boldsymbol{a}(\boldsymbol{y}) \cdot \nabla_{\boldsymbol{y}} u(\boldsymbol{y}) = b(\boldsymbol{y})u(\boldsymbol{y}) + c(\boldsymbol{y}), \qquad \boldsymbol{y} \in \Omega. \tag{2.2}$$

We will consider such problems in connection with boundary values

$$u(\boldsymbol{y}) = \phi(\boldsymbol{y}) \quad \text{for } \boldsymbol{y} \in \Gamma \subset \partial\Omega. \tag{2.3}$$

We remark that $\boldsymbol{a}\cdot\nabla$ in (2.2) is a *directional derivative* in direction $\boldsymbol{a}$ so that $\boldsymbol{a}\cdot\nabla u = bu+c$ describes the rate of change of u along integral curves of the field $\boldsymbol{a}$ (i.e. solution curves of the ODE $\boldsymbol{z}'(s) = \boldsymbol{a}(\boldsymbol{z}(s))$ – see fig. 2.1).

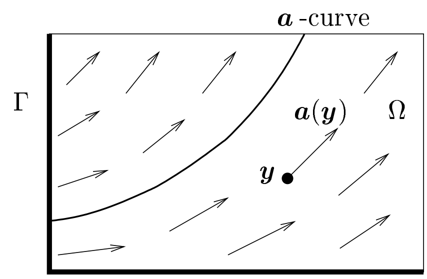

Figure 2.1 Integral curve of the vector field $\boldsymbol{a}$

More precisely, if $\boldsymbol{z}(s)$ is the solution of the ordinary differential equation $\boldsymbol{z}'(s) = \boldsymbol{a}(\boldsymbol{z}(s))$, we find

$$\frac{d}{ds}u(\boldsymbol{z}(s)) = \nabla u(\boldsymbol{z}(s)) \cdot \boldsymbol{a}(\boldsymbol{z}(s)) = b(\boldsymbol{z}(s))u(\boldsymbol{z}(s)) + c(\boldsymbol{z}(s)).$$

This simple observation is the basis for a solution method which is called the *method of characteristics*: In order to find a solution of equation (2.2) together with the boundary condition (2.3) in a point $\boldsymbol{y} \in \Omega$, we first have to find an $\boldsymbol{a}$-curve which connects $\boldsymbol{y}$ with a point $\bar{\boldsymbol{y}} \in \Gamma$ (fig. 2.2).

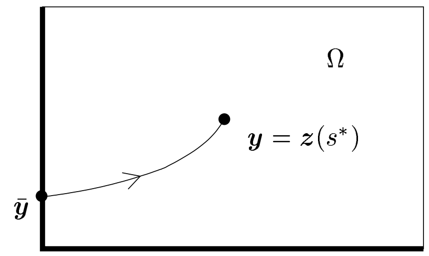

Figure 2.2 Integral curve connecting $\boldsymbol{y}$ with a boundary point $\bar{\boldsymbol{y}}$

In other words, we look for a solution $\boldsymbol{z}(s)$ of $\boldsymbol{z}'(s) = \boldsymbol{a}(\boldsymbol{z}(s))$ with the property $\boldsymbol{z}(0) = \bar{\boldsymbol{y}}$ and $\boldsymbol{z}(s^*) = \boldsymbol{y}$ (the curve $\boldsymbol{z}$ is called *characteristic ground curve*). Having found this curve, we use our knowledge about both the value $v(0) = \phi(\bar{\boldsymbol{y}})$ of the solution at the starting point, and the rate of change $v'(s) = b(\boldsymbol{z}(s))v(s) + c(\boldsymbol{z}(s))$ of the solution along $\boldsymbol{a}$-curves to compute the value $u(\boldsymbol{y}) = v(s^*)$ (fig. 2.3).

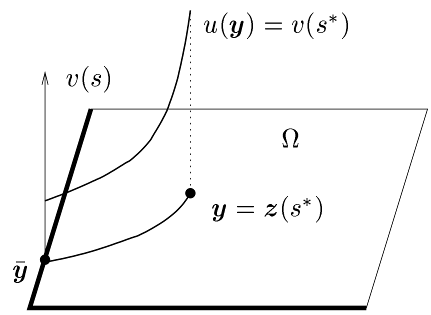

Figure 2.3 Values of the solution along the characteristic curve

Written in a compact form, the method of characteristics consists of three steps:

1) determine the solution $\boldsymbol{z}_{\bar{\boldsymbol{y}}}, v_{\bar{\boldsymbol{y}}}$ of the *characteristic system*

$$\begin{aligned} \boldsymbol{z}' &= \boldsymbol{a}(\boldsymbol{z}), \qquad & \boldsymbol{z}(0) &= \bar{\boldsymbol{y}} \\ v' &= b(\boldsymbol{z})v + c(\boldsymbol{z}), \qquad & v(0) &= \phi(\bar{\boldsymbol{y}}) \end{aligned}$$

2) find s^* and $\bar{\boldsymbol{y}} \in \Gamma$ such that $\boldsymbol{z}_{\bar{\boldsymbol{y}}}(s^*) = \boldsymbol{y}$

3) set $u(\boldsymbol{y}) = v_{\bar{\boldsymbol{y}}}(s^*)$.

We now consider several applications of this method.

2.1.1 Advection equation

The most simple application of the characteristic method is given by the advection equation (1.11) which we have found by linearizing the traffic flow model around the constant traffic density c

$$\frac{\partial u}{\partial t} + q'(c)\frac{\partial u}{\partial x} = 0, \quad u(0,x) = u^0(x).$$

Translating this equation into our general setup, we have $\boldsymbol{y} = (t,x)$, $\Omega = \mathbb{R}^+ \times \mathbb{R}$, $\Gamma = \partial\Omega$, $\phi(\boldsymbol{y}) = u^0(x)$, and $\boldsymbol{a}(\boldsymbol{y}) = (1,q'(c))$, $b = c = 0$. This leads to the characteristic system

$$\begin{aligned} \boldsymbol{z}' &= (1,q'(c)), \qquad & \boldsymbol{z}(0) &= (0,\bar{x}) \\ v' &= 0, & v(0) &= u^0(\bar{x}). \end{aligned}$$

Since the field $\boldsymbol{a}$ is independent of $\boldsymbol{y}$, the characteristic ground curves are straight lines (see fig. 2.4) and since $v' = 0$, the solution is constant along these lines.

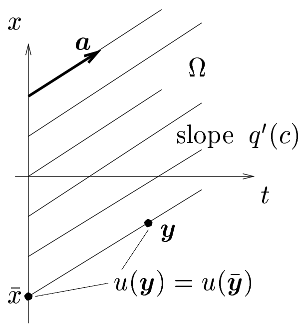

Figure 2.4 Characteristic ground curves for the advection equation

Formally, we have

1) the solution of the characteristic system

$$\boldsymbol{z}_{\bar{\boldsymbol{y}}}(s) = (s,\bar{x} + sq'(c)), \quad v_{\bar{\boldsymbol{y}}}(s) = u^0(\bar{x})$$

2) for $\boldsymbol{y} = (t,x) \in \Omega$ we have with $s^* = t$ and $\bar{x} = x - tq'(c)$ that $\boldsymbol{z}_{\bar{\boldsymbol{y}}}(s^*) = \boldsymbol{y}$

3) the solution has the form

$$u(t,x) = v_{\bar{\boldsymbol{y}}}(s^*) = u^0(x - tq'(c)).$$

Geometrically, the initial value $\boldsymbol{u}^0$ is simply advected with velocity $q'(c)$ (see fig. 2.5).

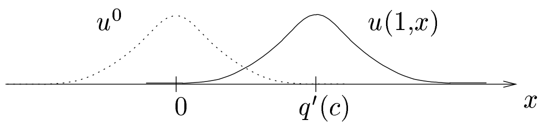

Figure 2.5 Solution of the advection equation at time $t = 1$

Note that the speed of transport $q'(c)$ is different from the car speed $V(c)$ since $q(u) = uV(u)$ so that $q'(c) = V(c) + cV'(c)$. Since V is typically a decreasing function (see fig. 1.5), $q'(c)$ will be less than $V(c)$ and can even be negative. This result coincides with the every-day observation that disturbances in the traffic density travel backwards along the road.

2.1.2 Stationary radiative transport

In radiative transport, the balanced quantity is the energy of radiation where

$$M(A \times B) = \int_A \int_B I(\boldsymbol{x},\boldsymbol{\xi})\, d\boldsymbol{\xi} d\boldsymbol{x}$$

is the energy in the domain $A \subset \mathbb{R}^d$ with ray directions $\boldsymbol{\xi} \in S^{d-1}$. The density $I(\boldsymbol{x},\boldsymbol{\xi})$ is called intensity. The rate of change of the intensity along rays is influenced by absorption (parameter $\sigma_a \geq 0$), scattering (e.g. isotropic with parameter $\sigma_s \geq 0$), and possible sources $\tilde{Q}$

$$\boldsymbol{\xi} \cdot \nabla I = -\sigma_a I - \sigma_s \left(I - \frac{1}{4\pi} \int_{S^2} I \, d\boldsymbol{\eta} \right) + \tilde{Q}.$$

To focus on the difficulties in the characteristic method, we assume $\sigma_s = 0$ and $\tilde{Q} = 0$. Then, with the combined variable $\boldsymbol{y} = (\boldsymbol{x},\boldsymbol{\xi})$, the characteristic system is based on $\boldsymbol{a}(\boldsymbol{y}) = (\boldsymbol{\xi},0)$ and $b(\boldsymbol{y}) = -\sigma_a$ and has the simple solution

$$\boldsymbol{z}_{\bar{\boldsymbol{y}}}(s) = (\bar{\boldsymbol{x}} + s\bar{\boldsymbol{\xi}},\bar{\boldsymbol{\xi}}), \quad v_{\bar{\boldsymbol{y}}}(s) = I(\bar{\boldsymbol{x}},\bar{\boldsymbol{\xi}})e^{-\sigma_a s}$$

where $\bar{\boldsymbol{y}} = (\bar{\boldsymbol{x}},\bar{\boldsymbol{\xi}})$ is a point on $\Gamma \subset \partial\Omega$. The more difficult task in the method of characteristics is given by the inversion problem: given some point $\boldsymbol{y} \in \Omega$, find the corresponding point $\bar{\boldsymbol{y}} = (\bar{\boldsymbol{x}},\bar{\boldsymbol{\xi}})$ on the boundary. This means that intersection points of straight lines (the characteristic ground curves) with, in general, curved boundaries have to be detected which can be quite complicated (see fig. 2.6).

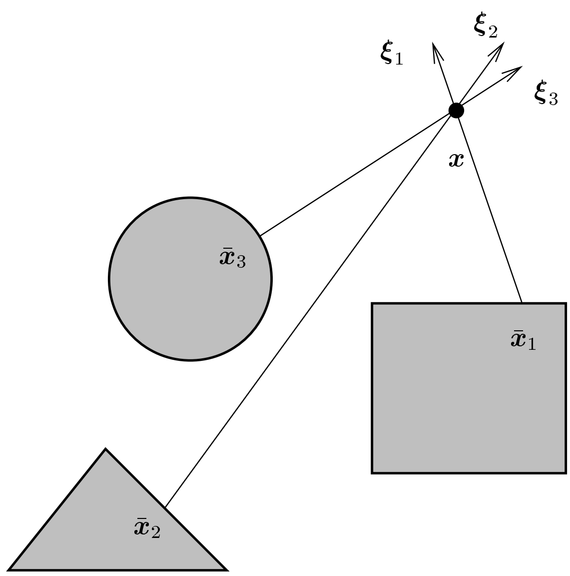

Figure 2.6 Intersection of rays with general boundaries in $\boldsymbol{x}$-space

To illustrate the phenomenon of non-smooth solutions, let us consider the following example: as spatial domain $\Omega^s \subset \mathbb{R}^2$, we take the annulus between the two circles $\Gamma_0^s = S^1$ and $\Gamma_1^s = RS^1$ with $R > 1$ (see fig. 2.7) which gives rise to the $\boldsymbol{y}$ -domain $\Omega = \Omega^s \times S^1$.

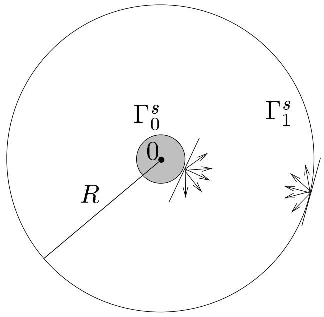

Figure 2.7 Spatial geometry of the radiation problem

The boundary on which we want to prescribe values consists of two parts

$$\Gamma_0 = \{(\boldsymbol{x},\boldsymbol{\xi}) : \boldsymbol{x} \in \Gamma_0^s, \boldsymbol{\xi} \in S^1, \boldsymbol{x} \cdot \boldsymbol{\xi} > 0\},$$
$$\Gamma_1 = \{(\boldsymbol{x},\boldsymbol{\xi}) : \boldsymbol{x} \in \Gamma_1^s, \boldsymbol{\xi} \in S^1, \boldsymbol{x} \cdot \boldsymbol{\xi} < 0\}.$$

On Γ_0 we assume Lambert radiation

$$I(\boldsymbol{x},\boldsymbol{\xi}) = I_0 \boldsymbol{x} \cdot \boldsymbol{\xi}, \quad (\boldsymbol{x},\boldsymbol{\xi}) \in \Gamma_0, \quad I_0 > 0$$

and on Γ_1 the (rather artificial) case of constant radiation in all directions

$$I(\boldsymbol{x},\boldsymbol{\xi}) = I_1, \quad (\boldsymbol{x},\boldsymbol{\xi}) \in \Gamma_1, \quad I_1 \geq 0.$$

Taking as parameters $R = 20$, $\sigma_a = 1/10$, $Q = 0$, $\sigma_s = 0$, $I_0 = 1$, and $I_1 = 0$, we calculate the solution at three different points in the domain (see fig. 2.8(a)).

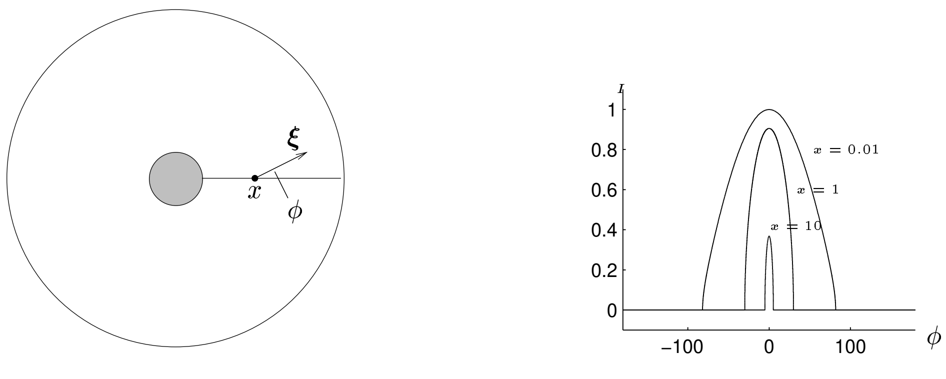

(a) Position x and angle ϕ (b) Intensity at different x

Figure 2.8 Solution of the radiation problem for background intensity $I_1 = 0$

For fixed $\boldsymbol{x} = (1 + x,0)$, the solution still depends on $\boldsymbol{\xi}$ which we express in terms of the angle ϕ (measured in degree in fig. 2.8(b)). Note that for increasing distance from the radiating surface Γ_0^s, the angle decreases in which radiation is received (the circle appears smaller in larger distance). Also, the maximal intensity decreases because of absorption. We also remark that the solution is not differentiable for all $\boldsymbol{\xi}$ because of the obvious jump in the slopes of the solution. This situation is even more pronounced, if we choose $I_1 > 0$ (see fig. 2.9).

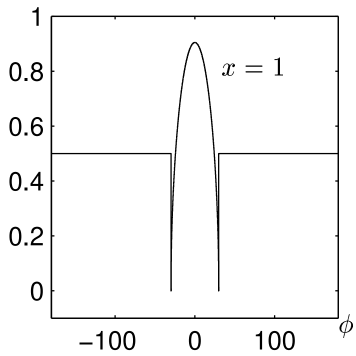

Figure 2.9 Solution of the radiation problem for background intensity $I_1 = 1/2$

Then, the solution is not even continuous despite the fact that all given data and boundaries are perfectly smooth. The reason for this behavior is explained schematically in fig. 2.10: we assume that along the curve Γ the very smooth data ϕ are prescribed and that the solution is constant along characteristic ground curves. Now consider the situation that one of the $\boldsymbol{a}$-curves starts in $\boldsymbol{y}^*$ and touches the boundary again in $\bar{\boldsymbol{y}}$ (i.e. $\boldsymbol{n}(\bar{\boldsymbol{y}}) \cdot \boldsymbol{a}(\bar{\boldsymbol{y}}) = 0$).

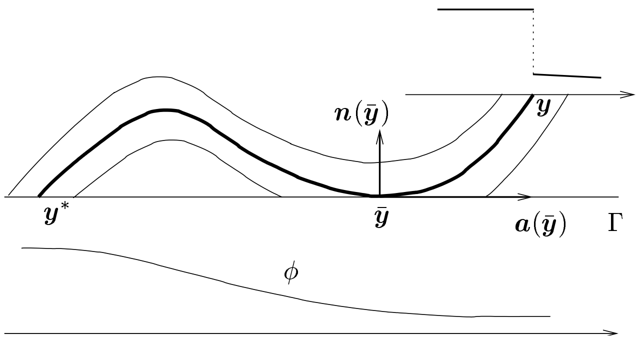

Figure 2.10 Discontinuous solution because of characteristic points on Γ

If we plot the solution in a neighborhood of $\boldsymbol{y} \in \Omega$ we see that curves which arrive left of the one which touches the boundary carry large values of ϕ while those on the right carry small values. Consequently, the solution has a jump in $\boldsymbol{y}$. This behavior is obviously caused by the geometric property of Γ to be parallel to $\boldsymbol{a}$ in the point $\bar{\boldsymbol{y}}$ (Γ is called *characteristic* in $\bar{\boldsymbol{y}}$). Note that prescribing data on surfaces which are characteristic at some points leads to solvability problems: on the one hand, the value of the solution in $\bar{\boldsymbol{y}}$ is given by $\phi(\bar{\boldsymbol{y}})$, on the other hand, it is given by $\phi(\boldsymbol{y}^*)$ because u is constant along characteristics in our example. This leads to a contradiction since $\phi(\bar{\boldsymbol{y}}) \neq \phi(\boldsymbol{y}^*)$ (the problem is actually shared by all points between $\boldsymbol{y}^*$ and $\bar{\boldsymbol{y}}$). We remark that the jump in the radiation problem (fig. 2.9) occurs exactly for those ray directions which belong to rays starting in $\boldsymbol{x}$ and being tangential to the small circle Γ_0^s . Note that such jumps are extremely important for the human visual orientation because they allow to distinguish between objects like the circle Γ_0^s and the background Γ_1^s .

2.1.3 Vlasov-equation with constant force

A straight forward application of the method of characteristics yields solutions of the initial value problem for the Vlasov equation (1.13) with constant force field

$$\frac{\partial f}{\partial t} + \boldsymbol{v} \cdot \nabla_{\boldsymbol{x}} f + \boldsymbol{g} \cdot \nabla_{\boldsymbol{v}} f = 0, \quad f(0,\boldsymbol{x},\boldsymbol{v}) = f^0(\boldsymbol{x},\boldsymbol{v})$$

Setting $\boldsymbol{y} = (t,\boldsymbol{x},\boldsymbol{v})$, $\Omega = \mathbb{R}^+ \times \mathbb{R}^3 \times \mathbb{R}^3$, $\Gamma = \partial\Omega$, we find the characteristic system with $\boldsymbol{a}(\boldsymbol{y}) = (1,\boldsymbol{v},\boldsymbol{g})$, $b = c = 0$. Since the boundary Γ has normal $\boldsymbol{n} = (-1,0,0)$, it is nowhere-characteristic and arbitrary boundary data f^0 can be described along Γ . The solution of the characteristic system has the form

$$\boldsymbol{z}(s) = (s,\bar{\boldsymbol{x}} + s\bar{\boldsymbol{v}} + s^2\boldsymbol{g}/2,\bar{\boldsymbol{v}} + s\boldsymbol{g}).$$

Solving $\boldsymbol{y} = (t,\boldsymbol{x},\boldsymbol{v}) = \boldsymbol{z}_{\bar{\boldsymbol{y}}}(s^*)$ for s^* and $\bar{\boldsymbol{y}}$, we eventually obtain

$$f(t,\boldsymbol{x},\boldsymbol{v}) = f^0(\boldsymbol{x} - t\boldsymbol{v} + t^2\boldsymbol{g}/2,\boldsymbol{v} - t\boldsymbol{g}).$$

2.1.4 Crystal precipitation

In the production of photographic paper or films, silver halide crystals (i.e. silver bromide, iodide, or chloride) of a certain size distribution are required (between 0.5 and 7 μm). We present a simple model for the prediction of crystal size distributions (taken from [4]).

Starting with a well stirred solution with salt concentration $c(t)$ at time t , we are interested in the number $M_t(I)$ of crystals with typical diameter $l \in I \subset \mathbb{R}^+$

$$M_t(I) = \int_I u(t,L)\,dL.$$

To describe the "transport" in the space of typical diameters, we assume that a crystal of size L at time t changes its size according to

$$\frac{dL}{dt} = G(t,L)$$

where we take the model of *Ostwald ripening*

$$G(t,L) = \begin{cases} k_g(c(t) - \exp(\alpha/L))^g & L \geq \alpha/\log c(t) \\ -k_d(\exp(\alpha/L) - c(t))^d & L < \alpha/\log c(t) \end{cases}$$

where $\alpha,k_g,k_d > 0$, $1 \leq g,d \leq 2$. For simplicity, we assume that there are no sources $(Q = 0)$ and we obtain the conservation law

$$\frac{\partial u}{\partial t} + \frac{\partial}{\partial L}(uG) = 0, \quad u(0,L) = u^0(L) > 0 \tag{2.4}$$

Note, however, that if crystals grow, they take salt atoms out of the solution. The mass used within the crystals (compared to the initial mass) is given by

$$\rho k_v \int_0^\infty L^3(u(t,L) - u^0(L))\, dL$$

where k_v is a parameter which relates the third power of the typical diameter to the volume of the crystal. Obviously, the consumed mass changes the salt concentration which satisfies

$$c(t) = c_0 - \rho k_v \int_0^\infty L^3(u(t,L) - u^0(L))\, dL \tag{2.5}$$

so that $c(t)$ depends on the solution u. Note that c enters in the formula for the flow velocity G so that the coupled system (2.4) and (2.5) is actually non-linear. A typical solution technique for such a problem is based on a fixed point formulation: we first assume that $c(t)$ is a *given* function and solve the (linear) problem (2.4) (for example, with the method of characteristics). Having obtained the solution u depending on the given function c, we define the map

$$P(c) = c_0 - \rho k_v \int_0^\infty L^3(u(t,L) - u^0(L))\, dL.$$

A solution of the non-linear problem is then given by the fixed point $P(c) = c$ and the corresponding solution of (2.4). A typical characteristic field for equation (2.4) is shown in fig. 2.11 where the concentration has been chosen as $c(t) = 2\exp(-t)$, $g = d = 1.5$, $k_g = k_d = 1.0$, $\alpha = 0.1$. One can distinguish two parts in the (t,L)-space. Above the thick curve, the crystals are growing and in the lower part crystals disappear.

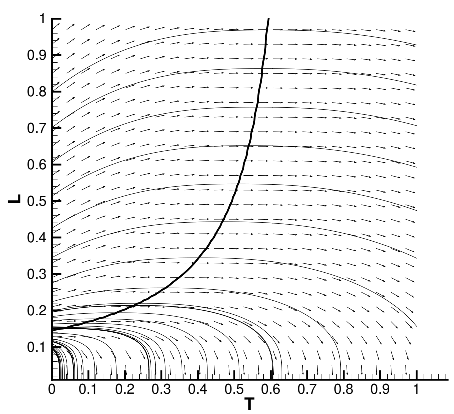

Figure 2.11 Characteristic ground curves for the crystal growth equation

2.2 Linear systems

We consider a system of conservation laws for the variables $\boldsymbol{U} = (U_1, \ldots, U_m)$

$$\frac{\partial U_i}{\partial t} + \operatorname{div}_{\boldsymbol{x}} \boldsymbol{q}_i(\boldsymbol{U}) = 0, \quad i = 1, \ldots, m.$$

The system is called linear if the fluxes $\boldsymbol{q}_i = (q_i^{(1)}, \ldots, q_i^{(d)})$ are linear in $\boldsymbol{U}$, i.e.

$$q_i^{(k)}(\boldsymbol{U}) = \sum_{j=1}^{m} a_{ij}^{(k)} U_j.$$

Introducing the matrices $A^{(k)} = (a_{ij}^{(k)})$, we can write the system in the form

$$\frac{\partial \boldsymbol{U}}{\partial t} + \sum_{k=1}^{d} A^{(k)} \frac{\partial \boldsymbol{U}}{\partial x_k} = 0. \tag{2.6}$$

A system of the form (2.6) is hyperbolic if all eigenvalues of the matrix $\sum_{k=1}^{d} \xi_k A^{(k)}$ are real for all $\boldsymbol{\xi} \in \mathbb{R}^d$. Considering the acoustics equations (1.23)

$$\frac{\partial p}{\partial t} + \operatorname{div} \boldsymbol{u} = 0, \quad \frac{\partial u_i}{\partial t} + \operatorname{div}(c^2 p \boldsymbol{e}_i) = 0 \tag{2.7}$$

with $c^2 = P'(\rho_0)$ and $\boldsymbol{e}_i$ being the i th unit vector, we can write (2.7) in the form (2.6) with

$$A^{(1)} = \begin{pmatrix} 0 & 1 & 0 & 0 \\ c^2 & 0 & 0 & 0 \\ 0 & 0 & 0 & 0 \\ 0 & 0 & 0 & 0 \end{pmatrix}, \quad A^{(2)} = \begin{pmatrix} 0 & 0 & 1 & 0 \\ 0 & 0 & 0 & 0 \\ c^2 & 0 & 0 & 0 \\ 0 & 0 & 0 & 0 \end{pmatrix}, \quad A^{(3)} = \begin{pmatrix} 0 & 0 & 0 & 1 \\ 0 & 0 & 0 & 0 \\ 0 & 0 & 0 & 0 \\ c^2 & 0 & 0 & 0 \end{pmatrix}$$

To check whether (2.7) is hyperbolic, we could try to calculate the eigenvalues of $\sum_{k=1}^{d} \xi_k A^{(k)}$ directly. However, one can use an important structure of (2.7) to show hyperbolicity.

2.2.1 Symmetric hyperbolic systems

If we multiply the acoustics equations written in general form (2.6) with the symmetric, positive definite (spd) matrix

$$B^{(0)} = \begin{pmatrix} c^2 & 0 & 0 & 0 \\ 0 & 1 & 0 & 0 \\ 0 & 0 & 1 & 0 \\ 0 & 0 & 0 & 1 \end{pmatrix}$$

from the left, we observe that the matrices $B^{(k)} = B^{(0)} A^{(k)}$ are symmetric

$$B^{(1)} = \begin{pmatrix} 0 & c^2 & 0 & 0 \\ c^2 & 0 & 0 & 0 \\ 0 & 0 & 0 & 0 \\ 0 & 0 & 0 & 0 \end{pmatrix}, \quad B^{(2)} = \begin{pmatrix} 0 & 0 & c^2 & 0 \\ 0 & 0 & 0 & 0 \\ c^2 & 0 & 0 & 0 \\ 0 & 0 & 0 & 0 \end{pmatrix}, \quad B^{(3)} = \begin{pmatrix} 0 & 0 & 0 & c^2 \\ 0 & 0 & 0 & 0 \\ 0 & 0 & 0 & 0 \\ c^2 & 0 & 0 & 0 \end{pmatrix}.$$

Hence, also linear combinations $\sum_{k=1}^{d} \xi_k B^{(k)} = B^{(0)} \sum_{k=1}^{d} \xi_k A^{(k)}$ are symmetric and from this property we can immediately conclude that $A = \sum_{k=1}^{d} \xi_k A^{(k)}$ has only real eigenvalues. To see this, we introduce a scalar product on $\mathbb{C}^m$

$$\left\langle B^{(0)} \boldsymbol{x}, \bar{\boldsymbol{y}} \right\rangle = \sum_{i,j} B_{ij}^{(0)} x_j \bar{y}_i$$

where the bar denotes complex conjugation. If $\boldsymbol{e} \in \mathbb{C}^m$ is an eigenvector of A with eigenvalue $\lambda \in \mathbb{C}$ and the normalization $\left\langle B^{(0)}\boldsymbol{e},\bar{\boldsymbol{e}}\right\rangle = 1$, we find

$$\lambda - \bar{\lambda} = \left\langle B^{(0)}\lambda\boldsymbol{e},\bar{\boldsymbol{e}}\right\rangle - \left\langle B^{(0)}\boldsymbol{e},\bar{\lambda}\bar{\boldsymbol{e}}\right\rangle .$$

Using the symmetry of $B^{(0)}$, we conclude further

$$\lambda - \bar{\lambda} = \left\langle B^{(0)}A\boldsymbol{e},\bar{\boldsymbol{e}}\right\rangle - \left\langle \boldsymbol{e},B^{(0)}A\bar{\boldsymbol{e}}\right\rangle$$

and with the symmetry of the product $B^{(0)}A$ it follows

$$\lambda - \bar{\lambda} = \left\langle B^{(0)}A\boldsymbol{e},\bar{\boldsymbol{e}}\right\rangle - \left\langle B^{(0)}A\boldsymbol{e},\bar{\boldsymbol{e}}\right\rangle = 0,$$

showing that λ is, in fact, real and that the acoustics equations are hyperbolic.

In general, one calls a system (2.6) *symmetric hyperbolic* if there exists a symmetric positive definite matrix $B^{(0)}$ such that all matrices $B^{(0)}A^{(k)}$ are symmetric. For systems having this structure, a complete existence and uniqueness theory is available, even in the case where the matrices depend on space and time (see [3]). A key feature which is used in the existence and uniqueness proofs are energy estimates which are obtained through an additional conservation law for the quantity

$$\eta(\boldsymbol{U}) = \frac{1}{2}\left\langle B^{(0)}\boldsymbol{U},\boldsymbol{U}\right\rangle$$

which is a convex function of $\boldsymbol{U}$. Indeed, if $\boldsymbol{U}$ is a solution of the symmetric hyperbolic system (2.6), we find with the symmetry assumptions

$$\begin{aligned}\frac{\partial\eta(\boldsymbol{U})}{\partial t} &= \left\langle B^{(0)}\boldsymbol{U},\frac{\partial\boldsymbol{U}}{\partial t}\right\rangle = -\left\langle B^{(0)}\boldsymbol{U},\sum_{k=1}^{d}A^{(k)}\frac{\partial\boldsymbol{U}}{\partial x_k}\right\rangle \\ &= -\left\langle \boldsymbol{U},\sum_{k=1}^{d}B^{(0)}A^{(k)}\frac{\partial\boldsymbol{U}}{\partial x_k}\right\rangle = -\sum_{k=1}^{d}\left\langle B^{(0)}A^{(k)}\boldsymbol{U},\frac{\partial\boldsymbol{U}}{\partial x_k}\right\rangle = -\sum_{k=1}^{d}\frac{\partial\phi_k(\boldsymbol{U})}{\partial x_k}\end{aligned}$$

where $\phi_k(\boldsymbol{U}) = \frac{1}{2}\left\langle B^{(0)}A^{(k)}\boldsymbol{U},\boldsymbol{U}\right\rangle$. In other words, the solution of a linear symmetric hyperbolic problem automatically satisfies the additional conservation law

$$\frac{\partial\eta(\boldsymbol{U})}{\partial t} + \mathrm{div}\phi(\boldsymbol{U}) = 0$$

with a strictly convex function η (note the similarity to the entropy concept for the Euler equation – in fact, if a hyperbolic system of conservation laws admits a strictly convex entropy, one can show that its linearizations are symmetric hyperbolic systems). In the case of system (2.7), the additional conserved quantity and its flux are

$$\eta(p,\boldsymbol{u}) = \frac{1}{2}c^2p^2 + \frac{1}{2}|\boldsymbol{u}|^2, \qquad \boldsymbol{\phi}(p,\boldsymbol{u}) = c^2p\boldsymbol{u}.$$

2.2.2 A problem with a moving boundary

In the following, we want to consider the linear equations of acoustics in a cylindrical tube with a moving piston on the left and a fixed wall on the right (see fig. 2.12).

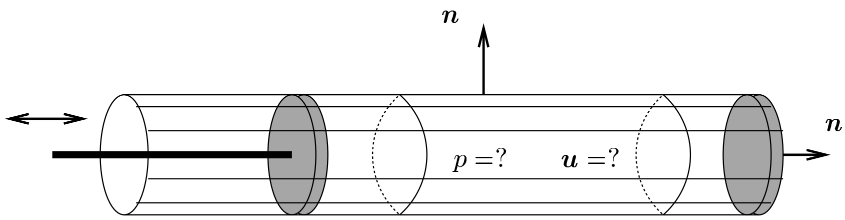

Figure 2.12 Model problem for the linear equations of acoustics

The piston movement will be prescribed as function $s(t)$ and we assume that all walls are impenetrable. If $\boldsymbol{n}$ is the outer normal field of this geometry, the boundary conditions lead to the equations $\boldsymbol{u} \cdot \boldsymbol{n} = -\dot{s}(t)$ on the piston and $\boldsymbol{u} \cdot \boldsymbol{n} = 0$ on the remaining walls. As initial condition we choose the constant state $p = p_0$, $\boldsymbol{u} = 0$. Because of axial symmetry, we look for a solution with the structure

$$p(x,y,z) = \hat{p}(x), \quad \boldsymbol{u}(x,y,z) = (\hat{u}(x),0,0), \quad x \in (s(t),1).$$

Plugging these expressions into the system (2.7), we obtain the one-dimensional problem

$$\begin{aligned} &\frac{\partial \hat{p}}{\partial t} + \frac{\partial \hat{u}}{\partial x} = 0, \quad \frac{\partial \hat{u}}{\partial t} + c^2 \frac{\partial \hat{p}}{\partial x} = 0 \\ &\hat{u}(0,x) = 0, \quad \hat{p}(0,x) = 1, \quad x \in (s(0),1) \\ &\hat{u}(t,s(t)) = \dot{s}(t), \quad \hat{u}(t,1) = 0, \quad t > 0. \end{aligned}$$

Note that, in case of uniqueness, a solution of the reduced system gives rise to the correct solution in three space dimensions.

Before we continue with the solution of the model problem, let us consider the general case of linear hyperbolic systems in a single space dimension

$$\frac{\partial \boldsymbol{U}}{\partial t} + A \frac{\partial \boldsymbol{U}}{\partial x} = 0, \quad (t,x) \in \Omega \tag{2.8}$$

where $\boldsymbol{U} = (U_1, \ldots, U_m)$. Assuming that we have a basis of eigenvectors of A

$$A\boldsymbol{r}_i = \lambda_i \boldsymbol{r}_i, \qquad i = 1, \ldots, m \tag{2.9}$$

we set up the matrices $R = (\boldsymbol{r}_1 \ldots \boldsymbol{r}_m)$ and $\Lambda = \mathrm{diag}(\lambda_1, \ldots, \lambda_m)$ such that (2.9) can be written as

$$R^{-1} A R = \Lambda.$$

If $\boldsymbol{U}$ is a solution of (2.8) one can show that the characteristic variables $\boldsymbol{\alpha} = R^{-1}\boldsymbol{U}$ solve a much simpler problem

$$\frac{\partial \boldsymbol{\alpha}}{\partial t} = R^{-1} \frac{\partial \boldsymbol{U}}{\partial t} = -R^{-1} A \frac{\partial \boldsymbol{U}}{\partial x} = -R^{-1} A R \frac{\partial \boldsymbol{\alpha}}{\partial x} = -\Lambda \frac{\partial \boldsymbol{\alpha}}{\partial x}$$

which are actually m decoupled advection equations

$$\frac{\partial \alpha_i}{\partial t} + \lambda_i \frac{\partial \alpha_i}{\partial x} = 0, \qquad i = 1, \ldots, m.$$

In particular, the pure initial value problem

$$\frac{\partial \boldsymbol{U}}{\partial t} + A\frac{\partial \boldsymbol{U}}{\partial x} = 0, \quad \boldsymbol{U}(0,x) = \boldsymbol{U}^0(x)$$

has the solution $\boldsymbol{U}(t,x) = R\boldsymbol{\alpha}(t,x)$ where

$$\alpha_i(t,x) = \alpha_i^0(x - t\lambda_i), \qquad \boldsymbol{\alpha}^0 = R^{-1}\boldsymbol{U}^0.$$

For more general boundary value problems we will still use the fact that α_i is constant along the characteristics with slope λ_i (see fig. 2.13).

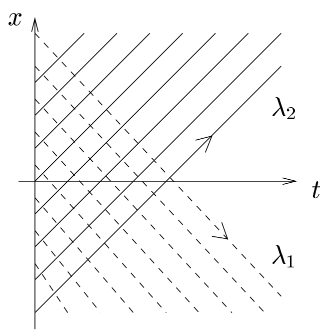

Figure 2.13 Characteristic ground curves for a system of two linear equations

Writing the reduced acoustic model in matrix vector form (and dropping the hat superscript), we get

$$\frac{\partial}{\partial t}\begin{pmatrix} p \\ u \end{pmatrix} + \begin{pmatrix} 0 & 1 \\ c^2 & 0 \end{pmatrix} \frac{\partial}{\partial x}\begin{pmatrix} p \\ u \end{pmatrix} = \begin{pmatrix} 0 \\ 0 \end{pmatrix} \tag{2.10}$$

The eigenvalues of the system matrix are $\lambda_1 = -c$, $\lambda_2 = +c$ with eigenvectors $\boldsymbol{r}_1 = (1,-c)$, $\boldsymbol{r}_2 = (1,c)$. This gives rise to the characteristic variables

$$\begin{pmatrix} \alpha_1 \\ \alpha_2 \end{pmatrix} = \begin{pmatrix} (p - u/c)/2 \\ (p + u/c)/2 \end{pmatrix}, \qquad \begin{pmatrix} p \\ u \end{pmatrix} = \begin{pmatrix} \alpha_2 + \alpha_1 \\ c(\alpha_2 - \alpha_1) \end{pmatrix} \tag{2.11}$$

The domain on which we want to solve (2.10) has the form as shown in fig. 2.14, if we assume that the piston follows a piecewise linear movement with speed $\pm 2A$.

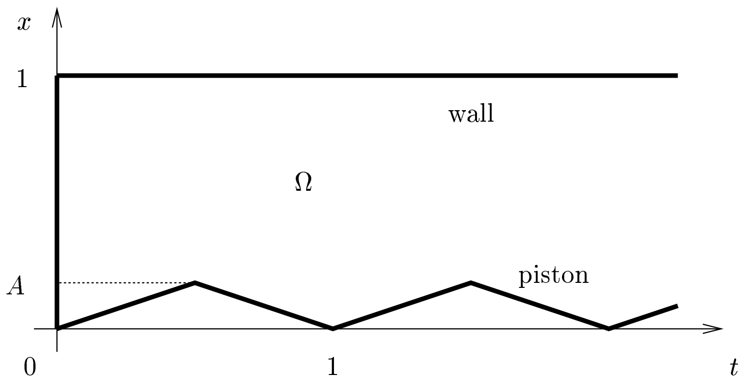

Figure 2.14 Geometry of the space time domain for the moving piston problem

Since $\lambda_1 < 0$, the characteristic curves of the first family run in negative x direction which means that α_1 is either determined by the initial values or by its values at the right wall (fig. 2.15).

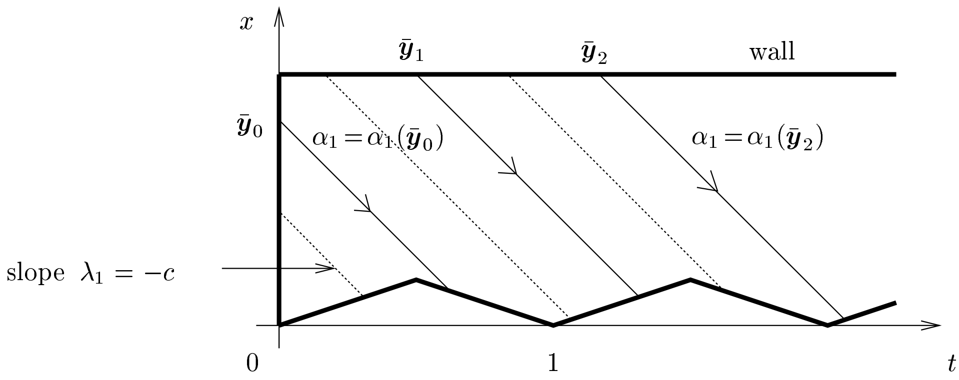

Figure 2.15 Lines along which α_1 is constant

Conversely, the characteristic curves of the second family run in positive x direction and α_2 is either determined by its value at the initial surface $t = 0$ or those at the moving boundary (see fig. 2.16).

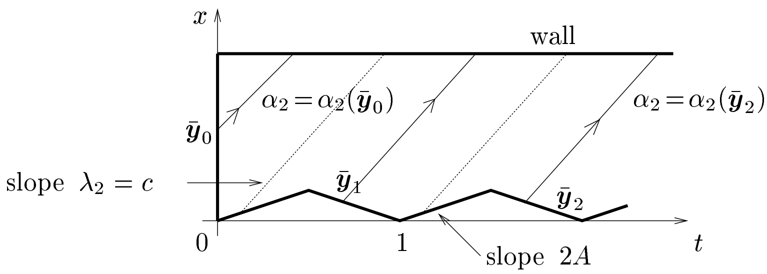

Figure 2.16 Lines along which α_2 is constant

At points $(\bar{t},\bar{x})$ of the left and the right x-boundary we have a condition of the form $u(\bar{t},\bar{x}) = v$ where $v = 0$ for $\bar{x} = 1$ and $v = \pm 2A$ for $\bar{x} = s(\bar{t})$. Using the transformation (2.11), this condition translates into $c(\alpha_2 - \alpha_1) = v$. Since the value of one of the variables α_1,α_2 is always available with the method of characteristics, the value of the other can be computed with the boundary data. Hence, the provided information suffices to solve the problem. As example, consider the situation depicted in fig. 2.17. To find the solution $p(\boldsymbol{y}),u(\boldsymbol{y})$, we need both α_1 and α_2 in the point $\boldsymbol{y} \in \Omega$.

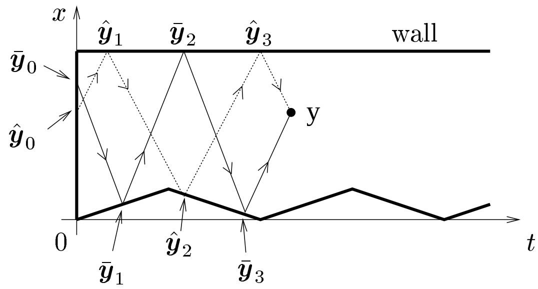

Figure 2.17 Solving the initial- boundary value problem with the method of characteristics

The value of α_1 is given by its value at $\hat{\boldsymbol{y}}_3$ which, according to the boundary condition is the same as $\alpha_2(\hat{\boldsymbol{y}}_3)$. To obtain $\alpha_2(\hat{\boldsymbol{y}}_3)$, we trace back the λ_2 -characteristic to the piston where we find $\alpha_2(\hat{\boldsymbol{y}}_3) = \alpha_2(\hat{\boldsymbol{y}}_2) = \alpha_1(\hat{\boldsymbol{y}}_2) - 2A/c$. Now, the missing value is $\alpha_1(\hat{\boldsymbol{y}}_2)$ which is equal to $\alpha_1(\hat{\boldsymbol{y}}_1)$ and finally we arrive at the initial surface $\alpha_1(\hat{\boldsymbol{y}}_1) = \alpha_2(\hat{\boldsymbol{y}}_1) = \alpha_2(\hat{\boldsymbol{y}}_0) = p_0/2$. For the value at $\boldsymbol{y}$ this implies $\alpha_1(\boldsymbol{y}) = p_0/2 - 2A/c$. The same procedure for α_2 yields $\alpha_2(\boldsymbol{y}) = p_0/2$ so that, after transforming α_1,α_2 into p,u

$$p(\boldsymbol{y}) = p_0 - \frac{2A}{c}, \qquad u(\boldsymbol{y}) = 2A.$$

Note that the switching between α_1 and α_2 at the boundaries corresponds to a wave reflection at the piston or wall respectively. We also remark that solvability problems arise if we prescribe, for example, velocity *and* pressure at the fixed wall. Since α_2 is already determined by the initial values or the values at the piston, it is, in general, not possible to enforce the values at the fixed wall. More generally, if we have a system of the form (2.8) in a domain Ω , we can prescribe in a point $\bar{\boldsymbol{y}} \in \partial\Omega$ only those characteristic variables α_i for which

$$\sigma \begin{pmatrix} 1 \\ \lambda_i \end{pmatrix} \cdot \boldsymbol{n}(\bar{\boldsymbol{y}}) < 0$$

where one has to choose $\sigma = 1$ for initial and $\sigma = -1$ for end-value problems. Geometrically, this means that values can only be prescribed for incoming characteristic curves (respectively outgoing characteristic curves in the case of end-value problems – see fig. 2.18).

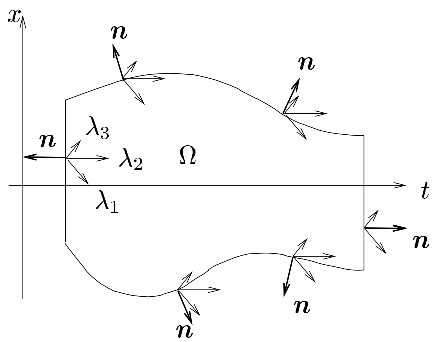

Figure 2.18 The number of incoming (outgoing) characteristic curves determines the number of boundary conditions

3 Weak solutions and entropy

Similar to the case of linear scalar balance laws, we rewrite the equation

$$\frac{\partial u}{\partial t} + \mathrm{div}_{\boldsymbol{x}} \boldsymbol{q} = Q$$

in divergence form using $\boldsymbol{y} = (t,\boldsymbol{x})$ and $\mathcal{A}(\boldsymbol{y},v) = (v,\boldsymbol{q}(\boldsymbol{y},v))$

$$\mathrm{div}_{\boldsymbol{y}} \mathcal{A}(\boldsymbol{y},u(\boldsymbol{y})) = Q(\boldsymbol{y},u(\boldsymbol{y})).$$

Setting $\boldsymbol{a}(\boldsymbol{y},v) = \frac{\partial}{\partial v}\mathcal{A}(\boldsymbol{y},v)$ and $b(\boldsymbol{y},v) = -\mathrm{div}_{\boldsymbol{y}} \mathcal{A}(\boldsymbol{y},v) + Q(\boldsymbol{y},v)$, we then obtain the quasilinear form

$$\boldsymbol{a}(\boldsymbol{y},u(\boldsymbol{y})) \cdot \nabla_{\boldsymbol{y}} u(\boldsymbol{y}) = b(\boldsymbol{y},u(\boldsymbol{y})), \qquad \boldsymbol{y} \in \Omega$$

which we consider in connection with boundary conditions $u(\boldsymbol{y}) = \phi(\boldsymbol{y})$ for $\boldsymbol{y} \in \Gamma \subset \Omega$. The difference to the linear case is now that the form of the characteristic ground curve depends also on the values of the solution along the curve, giving rise to the coupled characteristic system

$$\begin{aligned} \boldsymbol{z}' &= \boldsymbol{a}(\boldsymbol{z},v), & \qquad \boldsymbol{z}(0) &= \bar{\boldsymbol{y}} \\ v' &= b(\boldsymbol{z},v), & \qquad v(0) &= \phi(\bar{\boldsymbol{y}}). \end{aligned}$$

This coupling leads to the phenomenon that characteristic ground curves can cross in the nonlinear problem which is the breakdown of the characteristic method. The situation is illustrated in fig. 3.1 for the case $b = 0$ (i.e. u is constant along $\boldsymbol{a}$ curves).

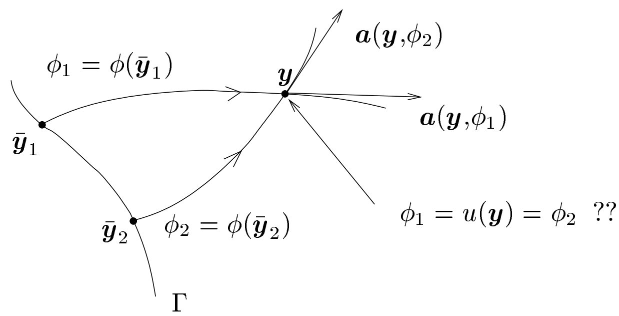

Figure 3.1 Characteristic ground curves can cross in the nonlinear case

If two characteristic ground curves cross in a point $\boldsymbol{y} \in \Omega$, it is impossible to trace back the value of u since ϕ_1 and ϕ_2 are generally different. To show that crossing characteristics appear naturally, we consider again the traffic flow model

$$\frac{\partial u}{\partial t} + \frac{\partial}{\partial x} q(u) = 0, \quad u(0,x) = u^0(x), \quad x \in \mathbb{R} \tag{3.1}$$

where $q(u) = uV(u)$ and $V(u)$ is the vehicle velocity. In order to completely specify the model, we adopt the simple choice shown in fig. 3.2(a), which at least gives qualitatively reasonable results.

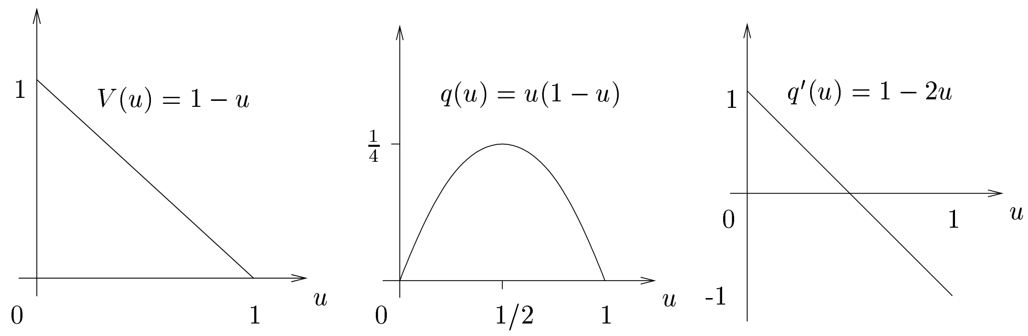

(a) vehicle velocity (b) traffic flux (c) flux derivative

Figure 3.2 Simple model for the density dependent vehicle velocity

Written in quasilinear form, equation (3.1) has the form $\boldsymbol{a}(u) \cdot \nabla u = 0$ with $\boldsymbol{a}(u) = (1,q'(u))$. The corresponding characteristic system

$$\boldsymbol{z}' = (1,q'(v)), \qquad \boldsymbol{z}(0) = (0,\bar{x})$$
$$v' = 0, \qquad v(0) = u^0(\bar{x})$$

has the solution $v(s) = u^0(\bar{x})$, $\boldsymbol{z}(s) = (s,\bar{x} + sq'(u^0(\bar{x})))$ and for the initial value u^0 shown in fig. 3.3(a), the characteristic ground curves are straight lines with different slopes which really cross in a certain subdomain of Ω (see fig. 3.3(b)).

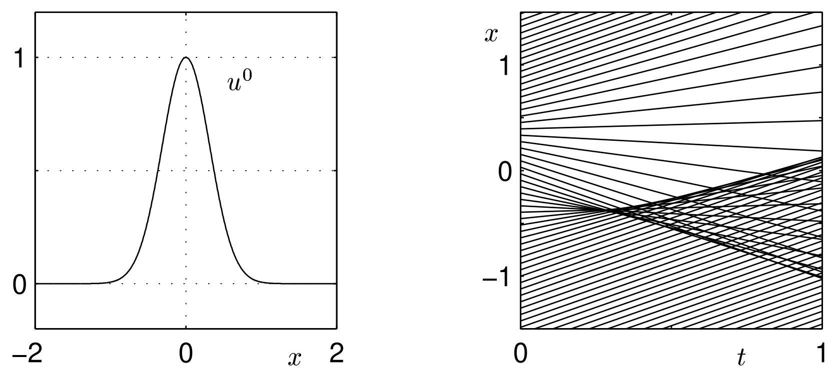

(a) Initial value (b) Characteristics

Figure 3.3 A typical initial value leading to crossing of characteristic ground curves

Solving (3.1) with the methods of characteristics therefore leads, after some time, to a multi-valued solution (see fig. 3.4(b)) which is unphysical because the traffic density along the road should be a single valued function.

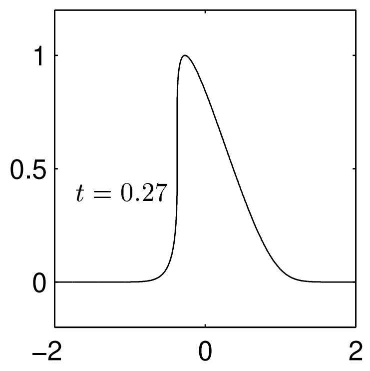

(a) $u(0.27,x)$

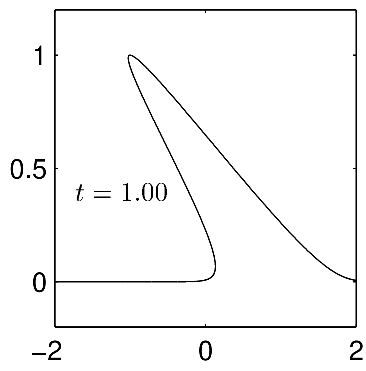

(b) $u(1.00,x)$

Figure 3.4 Solution of the method of characteristics for the initial value in fig. 3.3(a)

We will now show that the unexpected behavior of the model is related to the assumption that the vehicle speed is only a function of the traffic density. If we consider the acceleration felt by a vehicle at position $x(t)$ which is moving with speed $\dot{x}(t) = V(u(t,x(t)))$, we find

$$\ddot{x} = V'(u)\left(\frac{\partial u}{\partial t} + \dot{x}\frac{\partial u}{\partial x}\right) = (-1)\left(-q'(u)\frac{\partial u}{\partial x} + V(u)\frac{\partial u}{\partial x}\right) = -u\frac{\partial u}{\partial x} = -\frac{\partial}{\partial x}\left(\frac{1}{2}u^2\right)$$

Just before the failure of the characteristic method, it turns out that the density u exhibits a strong gradient (see fig. 3.4(a)) which even becomes infinite. In view of the expression for the acceleration, this means that the drivers have to break dramatically at the location of this strong increase which is due to the fact that they do not control their speed in view of the change in density ahead. On the other hand, the anticipation of the drivers is built into the refined model

$$\frac{\partial u_\alpha}{\partial t} + \frac{\partial}{\partial x}q(u_\alpha) = \alpha\frac{\partial^2 u_\alpha}{\partial x^2}, \quad u_\alpha(0,x) = u^0(x), \quad x \in \mathbb{R} \tag{3.2}$$

and it turns out that solutions of (3.2) do not show any unphysical behavior. Again, there is a formation of a steep gradient but it never exceeds a certain maximal slope (in fig. 3.5, the slope appears to be infinite only because of plotting accuracy).

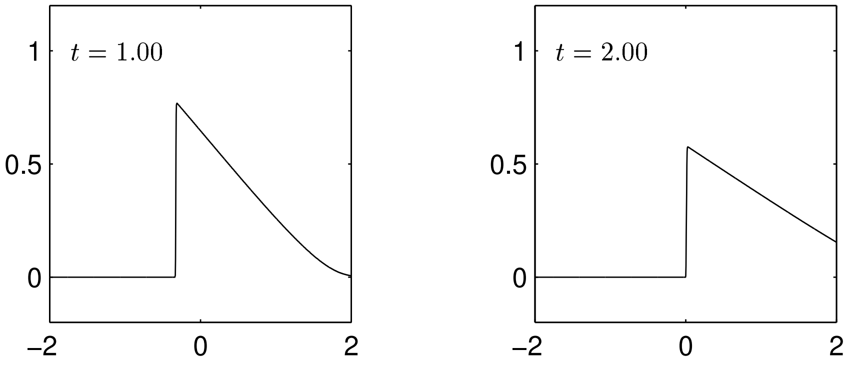

(a) $u(1.00,x)$ (b) $u(2.00,x)$

Figure 3.5 Solution of the model (3.2) with anticipating drivers and very small $\alpha > 0$

3.1 Weak solutions

Since we have introduced $\alpha > 0$ only as a small parameter to model the tendency that drivers react also on spatial variations in density, the question arises whether one can get rid of this parameter in the limit $\alpha \to 0$ while keeping the basic structure of the solution. Obviously, this limiting procedure cannot be carried out in the strong sense because $\|\partial_x q(u_\alpha)\|_{\mathbb{L}^\infty} \to \infty$ for $\alpha \to 0$. As remedy, we transform the equation (3.2) into a weak form in which the limit can be carried out safely. To do this, we first mention a quite general result about the divergence in the distributional sense.

Theorem 2 *Let $\Omega_1,\Omega_2 \subset \mathbb{R}^N$ be open, $\mathbb{R}^N = \bar{\Omega}_1 \cup \bar{\Omega}_2$, and let $\Gamma = \partial\Omega_1 = \partial\Omega_2$. Assume $\boldsymbol{w} : \mathbb{R}^N \to \mathbb{R}^N$ is a function whose restrictions $\boldsymbol{w}^{(i)} = \boldsymbol{w}|_{\Omega_i}$ are smooth such that the divergence theorem can be applied to $\Omega_i,\boldsymbol{w}^{(i)}$ (see fig. 3.6). Then, in the distributional sense, we have*

$$\mathrm{div}\boldsymbol{w} = \mathrm{div}^{(p)}\boldsymbol{w} + [\boldsymbol{w}] \cdot \boldsymbol{n}\delta_\Gamma \tag{3.3}$$

where $\mathrm{div}^{(p)}$ is the pointwise divergence defined in each subset Ω_i

$$\mathrm{div}^{(p)}\boldsymbol{w}(\boldsymbol{y}) = \begin{cases} \mathrm{div}\boldsymbol{w}^{(i)}(\boldsymbol{y}) & \boldsymbol{y} \in \Omega_i \\ 0 & \textit{else.} \end{cases}$$

The Distribution δ_Γ is defined by

$$\langle \delta_\Gamma,\psi \rangle = \int_\Gamma \psi(\boldsymbol{y})\, dS(\boldsymbol{y}), \qquad \forall \psi \in \mathscr{D}(\mathbb{R}^N)$$

and the jump $[\boldsymbol{w}]$ of $\boldsymbol{w}$ in the boundary points is given by

$$[\boldsymbol{w}](\boldsymbol{y}) = \lim_{s \searrow 0} \big(\boldsymbol{w}(\boldsymbol{y} + s\boldsymbol{n}(\boldsymbol{y})) - \boldsymbol{w}(\boldsymbol{y} - s\boldsymbol{n}(\boldsymbol{y}))\big) \quad \boldsymbol{y} \in \Gamma.$$

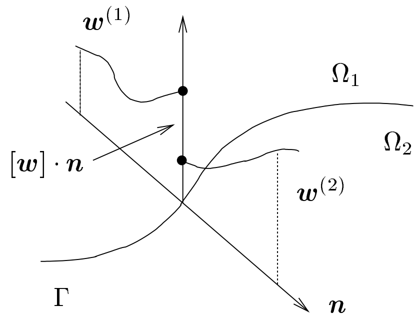

Figure 3.6 A piecewise smooth function with jump on the surface Γ

Proof: The proof relies on the divergence theorem. Taking any $\psi \in \mathscr{D}(\mathbb{R}^N)$, we have

$$
\begin{aligned}
\langle \mathrm{div}\boldsymbol{w},\psi\rangle &= -\sum_{j=1}^{N}\langle w_j,\partial_{x_j}\psi\rangle = -\sum_{k=1}^{2}\sum_{j=1}^{N}\int_{\Omega_k} w_j^{(k)}\partial_{x_j}\psi\, d\boldsymbol{y} \\
&= -\sum_{k=1}^{2}\int_{\Omega_k}\mathrm{div}(\psi\boldsymbol{w}^{(k)}) - \psi\mathrm{div}\boldsymbol{w}^{(k)}\, d\boldsymbol{y} \\
&= \sum_{k=1}^{2}\left(-\int_{\partial\Omega_k}\psi\boldsymbol{w}^{(k)}\cdot\boldsymbol{n}\, dS(\boldsymbol{y}) + \int_{\Omega_k}\psi\mathrm{div}\boldsymbol{w}^{(k)}\, d\boldsymbol{y}\right) \\
&= \int_{\Gamma}\psi(\boldsymbol{w}^{(2)}-\boldsymbol{w}^{(1)})\cdot\boldsymbol{n}\, dS(\boldsymbol{y}) + \int_{\mathbb{R}^N}\psi\mathrm{div}^{(p)}\boldsymbol{w}\, d\boldsymbol{y} \\
&= \left\langle [\boldsymbol{w}]\cdot\boldsymbol{n}\delta_\Gamma + \mathrm{div}^{(p)}\boldsymbol{w},\psi\right\rangle
\end{aligned}
$$

■

Using the divergence relation (3.3) of the above theorem, we can formulate (3.2) in the distributional sense. First, we extend the solution $u_\alpha(t,x)$ which is defined on $\Omega_2 = \{(t,x) : t > 0, x \in \mathbb{R}\}$ to the complement $\Omega_1 = \{(t,x) : t < 0, x \in \mathbb{R}\}$ by setting it equal to zero

$$
u_\alpha(t,x) = \begin{cases} 0 & t < 0 \\ u_\alpha(t,x) & t > 0 \end{cases}
$$

Using the space-time flux $\mathcal{A}(u_\alpha) = (u_\alpha, q(u_\alpha))$ we then conclude immediately

$$
\mathrm{div}_{\boldsymbol{y}}^{(p)}\mathcal{A}(u_\alpha) = \alpha\frac{\partial^2 u_\alpha}{\partial x^2}, \qquad \boldsymbol{y}\in\Omega_i, \quad i = 1,2.
$$

Moreover, on Γ_0 we have a jump in the normal component of $\mathcal{A}$ which is just given by the initial value

$$
[\mathcal{A}(u_\alpha)]\cdot\boldsymbol{n} = u^0 \quad \text{on } \Gamma_0.
$$

Using (3.3) we thus get in the sense of distributions

$$
\mathrm{div}_{(t,x)}\mathcal{A}(u_\alpha) = \alpha\frac{\partial^2 u_\alpha}{\partial x^2} + u^0\delta_{\Gamma_0} \qquad \text{in } \mathscr{D}'(\mathbb{R}^2)
$$

which means that for all $\psi \in \mathscr{D}(\mathbb{R}^2)$

$$-\int_{\mathbb{R}^2} \mathcal{A}(u_\alpha) \cdot \nabla\psi \, d\boldsymbol{y} = \alpha \int_{\mathbb{R}^2} u_\alpha \frac{\partial^2 \psi}{\partial x^2} \, d\boldsymbol{y} + \int_{\Gamma_0} u^0 \psi \, dS(\boldsymbol{y})$$

In this weak formulation of the problem, the limit $\alpha \to 0$ can be carried out under the mild assumption that $\|u_\alpha\|_{\mathbb{L}^\infty}$ is uniformly bounded and that $u_\alpha \to u$ almost everywhere. The limit of the solutions u_α then satisfies the condition

$$-\int_{\mathbb{R}^2} \mathcal{A}(u) \cdot \nabla\psi \, d\boldsymbol{y} = \int_{\Gamma_0} u^0 \psi \, dS(\boldsymbol{y}) \qquad \forall \psi \in \mathscr{D}(\mathbb{R}^2)$$

or, in the distributional sense, $\operatorname{div}_{(t,x)} \mathcal{A}(u) = u^0 \delta_{\Gamma_0}$. This observation gives rise to the definition of an extended solution concept for the hyperbolic problem

$$\frac{\partial u}{\partial t} + \frac{\partial}{\partial x} q(u) = 0, \qquad u(0,x) = u^0(x). \tag{3.4}$$

Definition 3 *Let* $u^0 \in \mathbb{L}^\infty(\mathbb{R})$, $u \in \mathbb{L}^\infty_{loc}(\mathbb{R}^2)$, $u(t,x) = 0$ *for* $t < 0$, $\Gamma_0 = \{0\} \times \mathbb{R}$. *Then, the function* u *is called weak solution of* (3.4), *provided*

$$\operatorname{div}_{(t,x)} \mathcal{A}(u) = u^0 \delta_{\Gamma_0} \quad \textit{in } \mathscr{D}'(\mathbb{R}^2)$$

We remark that classical solutions are automatically weak solutions which is an easy consequence of the divergence relation (3.3). In fact, if u is a classical solution of (3.4) then $\operatorname{div}^{(p)} \mathcal{A}(u) = 0$ and thus $\operatorname{div} \mathcal{A}(u) = u^0 \delta_{\Gamma_0}$ in $\mathscr{D}'$ which is the condition on u to be a weak solution. More generally, one can show with the same argument that a piecewise classical solution is a weak solution if and only if $[\mathcal{A}(u)] \cdot \boldsymbol{n} = 0$ on the jump line Γ_s (see fig. 3.7).

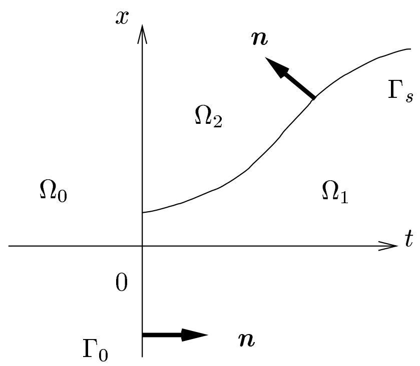

Figure 3.7 A piecewise classical solution is a weak solution if $[\mathcal{A}(u)] \cdot \boldsymbol{n} = 0$ on Γ_s

The proof of the statement again relies on the divergence relation (but now for the case of at least three sets Ω_i). Since the function u is a piecewise classical solution if and only if $\operatorname{div}^{(p)} \mathcal{A}(u) = 0$ in each subset, the relation

$$\operatorname{div}_{(t,x)} \mathcal{A}(u) = \operatorname{div}^{(p)} \mathcal{A}(u) + [\mathcal{A}(u)] \cdot \boldsymbol{n} \delta_{\Gamma_s} + u^0 \delta_{\Gamma_0} \quad \text{in } \mathscr{D}'(\mathbb{R}^2)$$

yields the condition $[\mathcal{A}(u)] \cdot \boldsymbol{n} = 0$ on Γ_s on u to be a weak solution. The jump condition $[\mathcal{A}(u)] \cdot \boldsymbol{n} = 0$ is called *Rankine-Hugoniot condition* and can be reformulated if we parameterize Γ_s according to

$$\Gamma_s = \{(t, s(t)) : t \in I\}, \qquad I = (\bar{t}, T).$$

Since the tangential vector on Γ_s is given by $\boldsymbol{\tau} = n_x(1, -n_t/n_x)$ (see fig. 3.8), the slope of s is given by $\dot{s} = -n_t/n_x$.

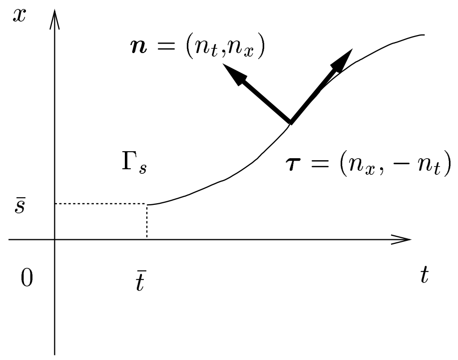

Figure 3.8 Normal and tangential vector at a point on the jump line

Hence $0 = [\mathcal{A}(u)] \cdot \boldsymbol{n} = [u]n_t + [q(u)]n_x$ implies the following condition on the so called shock curve s

$$\dot{s}(t) = \frac{[q(u)]}{[u]}(t,s(t)), \qquad s(\bar{t}) = \bar{s}.$$

This ordinary differential equation can be explicitly solved for our traffic flow model with $V(u) = 1 - u$, if we use a piecewise linear initial value as shown in fig. 3.9(a).

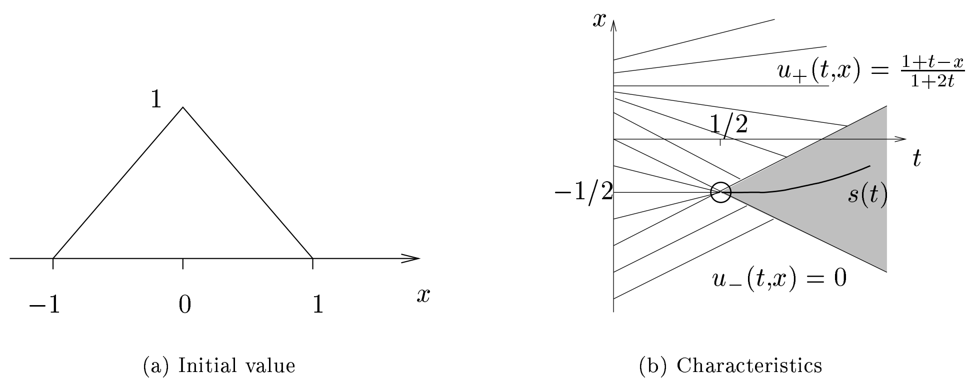

Figure 3.9 Shock solution for a piecewise linear initial condition

One easily finds out that the characteristic ground curves intersect for the first time in $\bar{s} = -1/2$ at $\bar{t} = 1/2$. In the conical shaped domain emanating from $(\bar{t},\bar{s})$ in fig. 3.9(b), one finds two possible classical solutions with the method of characteristics which are

$$u_-(t,x) = 0, \qquad u_+(t,x) = \frac{1+t-x}{1+2t}.$$

This leads to the ordinary differential equation

$$\dot{s}(t) = \frac{q(u_+) - q(u_-)}{u_+ - u_-}(t,s(t)) = \frac{t + s(t)}{1+2t}, \qquad s(1/2) = -1/2$$

which has the solution $s(t) = 1 + t - \sqrt{2 + 4t}$ for $t > 1/2$.

While the concept of weak solutions allows to cope with shock solutions, additional problems arise if uniqueness of weak solutions is considered. To give an example, we consider the initial value shown in fig. 3.10(a).

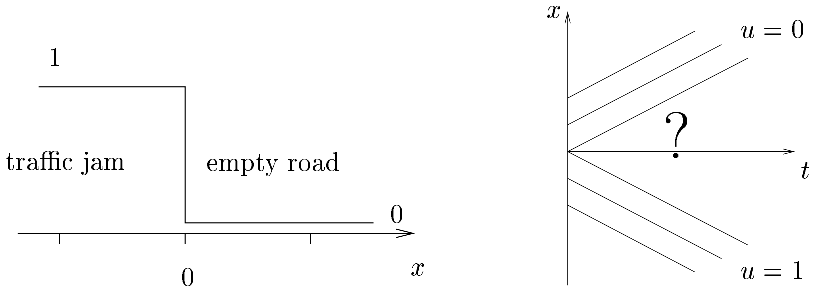

(a) Initial value (b) Characteristics

Figure 3.10 Characteristic ground curves leave a gap in (t,x) space

Since $q'(u) = 1 - 2u \in \{-1,1\}$ for $u \in \{0,1\}$, the characteristic ground curves leave a conical gap emanating from $(t,x) = (0,0)$ (fig. 3.10(b)). One method to fill this gap is to set $u(t,x) = 0$ for $x > 0$ and $u(t,x) = 1$ for $x < 0$. The jump surface $\Gamma_s = \{(t,0) : t > 0\}$ is then a valid shock surface because $[q(u)]/[u] = 0$ on Γ_s. Practically, the solution constructed in this way is stationary which means that no car in the traffic jam starts moving although the street is completely empty for $x > 0$ (see fig. 3.11(a)).

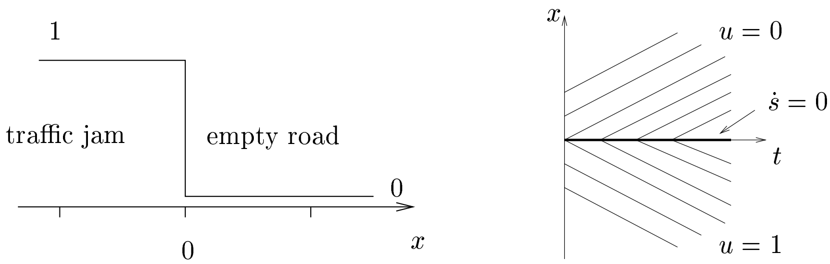

(a) Solution for $t > 0$ (b) Shock curve

Figure 3.11 Stationary shock solution for a piecewise constant initial condition

This very unrealistic behavior again seems to be the result of non-anticipating drivers. A different weak solution of the same problem, on the other hand, is much more reasonable. In fact, we can find a continuous weak solution of the problem by trying the ansatz $u(t,x) = \tilde{u}(x/t)$. Plugging this form into (3.1), we find the condition

$$\tilde{u}'(\xi)(q'(\tilde{u}(\xi)) - \xi) = 0, \qquad \xi = \frac{x}{t}$$

which is obviously satisfied for all ξ if

$$\tilde{u}(\xi) = (q')^{-1}(\xi) = \frac{1-\xi}{2}.$$

Since $\tilde{u}(1) = 0$ and $\tilde{u}(-1) = 1$, we therefore obtain a piecewise classical solution of the initial value problem by setting

$$u(t,x) = \begin{cases} 1 & x/t < -1 \\ (1-\xi)/2 & -1 \le x/t \le 1 \\ 0 & x/t > 1 \end{cases}$$

Note that u is a weak solution because it is piecewise classical and satisfies the jump condition $[\mathcal{A}(u)] \cdot \boldsymbol{n} = 0$ across the lines $x/t = \pm 1$, in fact, because of continuity we even have $[\mathcal{A}(u)] = 0$. This type of solution (see fig. 3.12(a)) is called *rarefaction wave.* It is characterized by the fact that it appears as limit of the solutions u_α of (3.2) for $\alpha \to 0$.

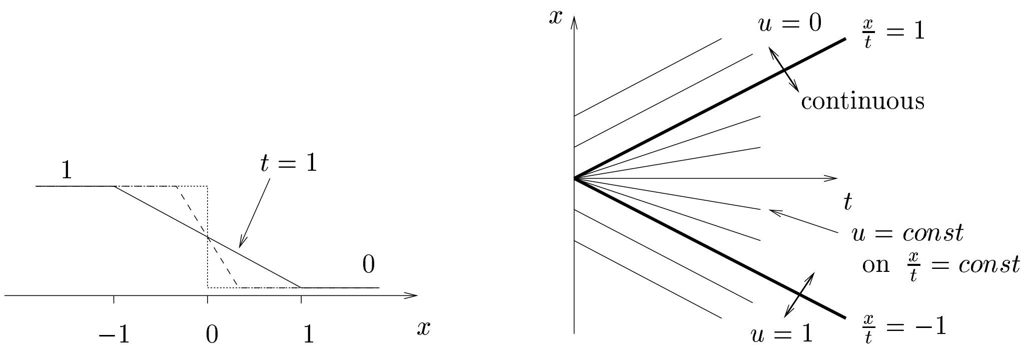

(a) Solutions for $t > 0$ (b) Characteristics

Figure 3.12 Rarefaction solution for a piecewise constant initial condition

3.2 Entropy condition

Since we accepted the model of the anticipating driver as a guiding line for the reduced model, it is natural to adopt the rarefaction solution and to discard the unrealistic shock solution. Unfortunately, the criterion to accept only the unique weak solution of (3.4) which is the limit of u_α for $\alpha \to 0$ is difficult to handle in practice. A more useful approach is given by the *entropy condition* which we will describe in the following. Let $\eta \in C^1(\mathbb{R})$ be a convex function (an *entropy*) and let ϕ be a primitive of $\eta' q'$ (an *entropy flux*). The pair $\mathcal{E}(u) = (\eta(u), \phi(u))$ is then called entropy-entropy flux pair and satisfies the relation

$$\mathcal{E}'(u) = \eta'(u)(1, q'(u)) = \eta'(u)\mathcal{A}'(u)$$

In particular, any classical solution of the hyperbolic conservation law $\mathrm{div}_{\boldsymbol{y}}\mathcal{A}(u) = 0$ satisfies automatically

$$\mathrm{div}_{\boldsymbol{y}}\mathcal{E}(u) = \mathcal{E}'(u) \cdot \nabla_{\boldsymbol{y}} u = \eta'(u)\mathcal{A}'(u) \cdot \nabla_{\boldsymbol{y}} u = \eta'(u)\mathrm{div}_{\boldsymbol{y}}\mathcal{A}(u) = 0 \tag{3.5}$$

which is an additional conservation law

$$\frac{\partial \eta(u)}{\partial t} + \frac{\partial \phi(u)}{\partial x} = 0.$$

Similarly, one obtains for the extended model (3.2)

$$\mathrm{div}_{\boldsymbol{y}} \mathcal{E}(u_\alpha) = \eta'(u_\alpha) \mathrm{div}_{\boldsymbol{y}} \mathcal{A}(u_\alpha) = \alpha \eta'(u_\alpha) \frac{\partial^2 u_\alpha}{\partial x^2}.$$

Since η is convex, we also have

$$\frac{\partial^2 \eta(u_\alpha)}{\partial x^2} = \underbrace{\eta''(u_\alpha)}_{\geq 0} \underbrace{\left(\frac{\partial u_\alpha}{\partial x}\right)^2}_{\geq 0} + \eta'(u_\alpha) \frac{\partial^2 u_\alpha}{\partial x^2}$$

so that altogether

$$\mathrm{div} \mathcal{E}(u_\alpha) \leq \alpha \frac{\partial^2 \eta(u_\alpha)}{\partial x^2}.$$

Extending again u_α according to

$$u_\alpha(t,x) = \begin{cases} 0 & t < 0 \\ u_\alpha(t,x) & t > 0 \end{cases}$$

we obtain in the distributional sense

$$\mathrm{div}_{\boldsymbol{y}} \mathcal{E}(u_\alpha) \leq \alpha \frac{\partial^2 \eta(u_\alpha)}{\partial x^2} + \eta(u^0) \delta_{\Gamma_0} \quad \text{in } \mathscr{D}'(\mathbb{R}^2)$$

which means more explicitly

$$-\int_{\mathbb{R}^2} \mathcal{E}(u_\alpha) \cdot \nabla_{\boldsymbol{y}} \psi \, d\boldsymbol{y} \leq \alpha \int_{\mathbb{R}^2} \eta(u_\alpha) \frac{\partial^2 \psi}{\partial x^2} \, d\boldsymbol{y} + \int_{\Gamma_0} \eta(u^0) \psi \, dS(\boldsymbol{y})$$

for all $\psi \in \mathscr{D}(\mathbb{R}^2)$ with $\psi \geq 0$. If $\|u_\alpha\|_{\mathbb{L}^\infty}$ is uniformly bounded and $u_\alpha \to u$ almost everywhere, we find that the limit u is a weak solution of (3.4) which satisfies for every convex entropy-entropy flux pair $\mathcal{E}$ the additional relation

$$\mathrm{div}_{\boldsymbol{y}} \mathcal{E}(u) \leq \eta(u^0) \delta_{\Gamma_0} \quad \text{in } \mathscr{D}'(\mathbb{R}^2)$$

It turns out that this *entropy condition* really singles out a unique weak solution among all possible weak solutions which is then, of course, the limit of the refined model (3.2) for $\alpha \to 0$. More precisely, one has the general result (for a proof see [8])

Theorem 4 *Let $u^0 \in \mathbb{L}^\infty(\mathbb{R})$ and $q \in C^1(\mathbb{R})$. Then there exists exactly one weak solution of*

$$\frac{\partial u}{\partial t} + \frac{\partial}{\partial x} q(u) = 0, \quad u(0,x) = u^0(x), \quad x \in \mathbb{R},$$

which satisfies $\mathrm{div}_{(t,x)} \mathcal{E}(u) \leq \eta(u^0) \delta_{t=0}$ in $\mathscr{D}'(\mathbb{R}^2)$ for all convex entropy-entropy flux pairs $\mathcal{E}$.

For the particular case of piecewise classical solutions, the entropy condition can be cast in a form similar to the Rankine-Hugoniot condition. More precisely, a piecewise classical solution satisfies the entropy condition if for all convex entropy-entropy flux pairs the jump condition $[\mathcal{E}(u)] \cdot \boldsymbol{n} \leq 0$ is satisfied on the shock curves Γ_s. The proof again relies on the divergence relation (3.3)

$$\operatorname{div}_{\boldsymbol{y}} \mathcal{E}(u) = \operatorname{div}^{(p)} \mathcal{E}(u) + [\mathcal{E}(u)] \cdot \boldsymbol{n} \delta_{\Gamma_s} + \eta(u^0) \delta_{\Gamma_0}$$

and on the fact that for piecewise classical solutions $\operatorname{div}^{(p)} \mathcal{E}(u) = 0$ according to (3.5). An additional consideration allows to restrict the entropy requirement to special entropy-entropy flux pairs of the form

$$\mathcal{E}_k(u) = \big(|u-k|, \operatorname{sign}(u-k)(q(u)-q(k)) \big), \quad k \in \mathbb{R}$$

(for details see [5]). Using the pairs $\mathcal{E}_k$ and the condition $[\mathcal{E}_k(u)] \cdot \boldsymbol{n} \leq 0$, elementary considerations show that a piecewise classical solution with jump *upwards* (see fig. 3.13(a)) satisfies the entropy condition if and only if the flux function $q(u)$ lies *above* the chord between $q(u_-)$ and $q(u_+)$ (fig. 3.13(b)).

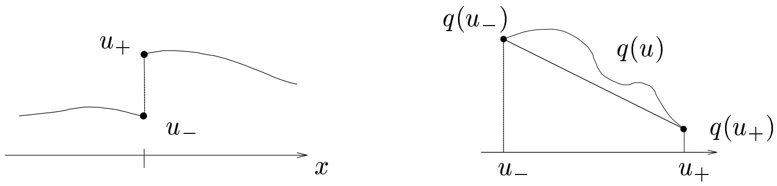

(a) Jump upwards (b) Flux function

Figure 3.13 Entropy condition for jumps upward

Conversely, a weak piecewise classical solution with jump *downward* (see fig. 3.14(a)) satisfies the entropy condition exactly when the flux function $q(u)$ lies *below* the chord between $q(u_+)$ and $q(u_-)$ (fig. 3.14(b)).

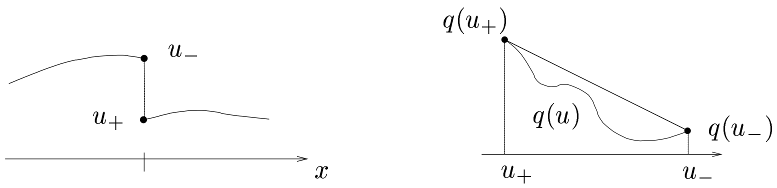

(a) Jump downwards (b) Flux function

Figure 3.14 Entropy condition for jumps downward

In the case of traffic flow, the flux function $q(u) = u(1-u)$, $u \in [0,1]$ is concave so that only jumps upwards can be entropy consistent. Equivalently, one can cast this condition in the form $q'(u_-) \geq \dot{s} \geq q'(u_+)$ which also holds in the case of convex fluxes and which has the nice geometrical interpretation of characteristic curves running into the shock (see fig. 3.15).

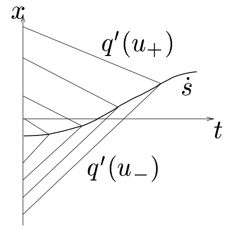

Figure 3.15 Characteristic curves running into the shock curve

3.3 Ion etching in semiconductor production

We consider an industrial application of a hyperbolic conservation law with a flux function which is neither convex nor concave. The example arises in connection with ion etching where a material (e.g. the semiconductor material GaAs) is etched at its surface by bombardment with a beam of ions (see fig. 3.16(a)).

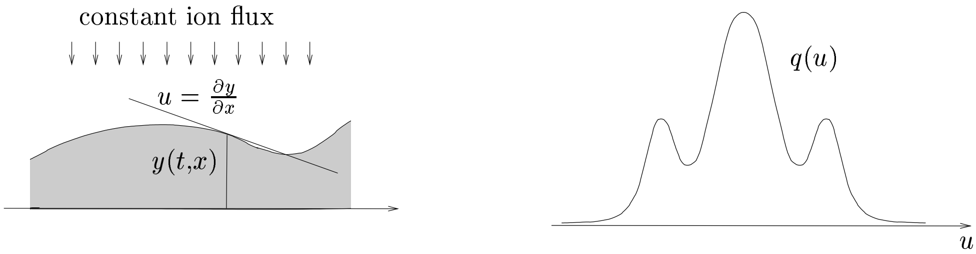

(a) The setup (b) Sputtering function

Figure 3.16 Etching of a material surface with a beam of ions

The removal of semiconductor material is proportional to the slope $u(t,x) = \frac{\partial y}{\partial x}$ of the surface $y(t,x)$ which leads to the evolution

$$\frac{\partial y}{\partial t} = -q\left(\frac{\partial y}{\partial x}\right) \tag{3.6}$$

The function q may have shapes as shown in fig. 3.16(b) where multiple local extrema can be caused by the crystalline structure of the semiconductor material. While (3.6) is a Hamilton-Jacobi equation for y, it can be transformed into a conservation law by going over to the x-derivative $u(t,x)$ of $y(t,x)$ which satisfies

$$\frac{\partial u}{\partial t} + \frac{\partial}{\partial x} q(u) = 0, \quad u(0,x) = y_0'(x) = u^0(x). \tag{3.7}$$

In the following, we will consider the Riemann problem consisting of equation (3.7) with initial value of jump type

$$u^0(x) = \begin{cases} u_- & x < 0 \\ u_+ & x > 0 \end{cases}$$

In terms of the semiconductor surface, upward jumps $u_+ > u_-$ correspond to configurations as in fig. 3.17(a) and downward jumps $u_+ < u_-$ to situations as in fig. 3.17(b). Before going into details of the ion etching example, we mention a general property of the unique entropy solution u of a Riemann problem. Setting $u_\beta(t,x) = u(\beta t,\beta x)$ for some $\beta > 0$, it is easily checked that u_β is also an entropy solution which implies that $u = u_\beta$ (because of uniqueness).

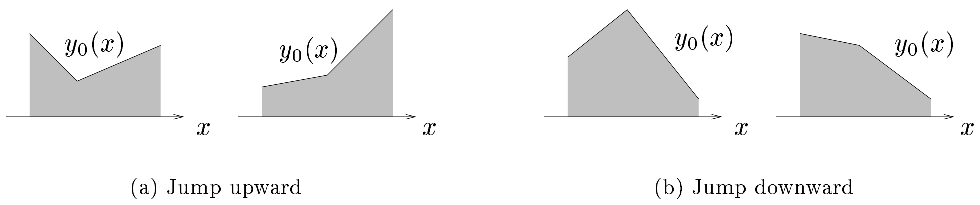

Figure 3.17 Geometric meaning of Riemann initial data for the slope of the surface

In particular, for some fixed $(\bar{t},\bar{x})$ we find

$$u(\bar{t},\bar{x}) = u_{1/\bar{t}}(\bar{t},\bar{x}) = u(1,\bar{x}/\bar{t}).$$

This result shows that the solution of the Riemann problem depends only on the quotient x/t (self similarity). Hence, it suffices to consider the solution at $t = 1$.

Let us now consider a jump upwards as initial value for equation (3.7) with flux function q shown in fig. 3.18(b).

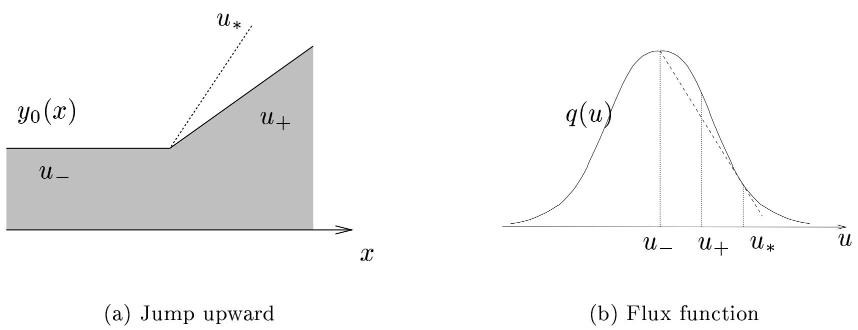

Figure 3.18 Riemann initial value for the ion etching equation

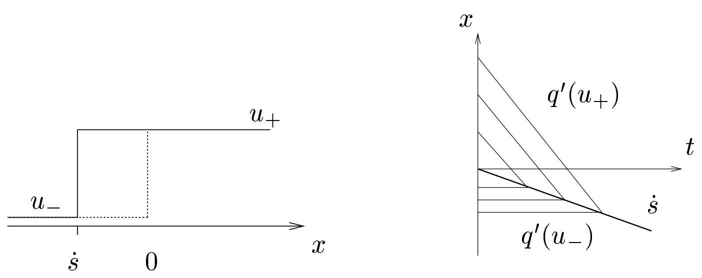

(a) Solution (b) Characteristics

Figure 3.19 Entropy solution for the initial value in fig. 3.18(a)

We first assume that the value u_- is zero and u_+ is chosen such that the chord between $q(u_-)$ and $q(u_+)$ is below the flux function $q(u)$ on the interval $[u_-,u_+]$ (the maximal u_+ satisfying this property is called u_*). According to the entropy condition, the correct entropy solution is then given by a shock which runs into negative x direction because $[q(u)]/[u] < 0$ (see fig. 3.19(a)). The effect of the moving jump discontinuity on the slope of the surface is obtained by integration

$$y(t,x) = y(t,\bar{x}) + \int_{\bar{x}}^{x} u(t,\sigma)\, d\sigma \tag{3.8}$$

where the height of the surface at the fixed point $\bar{x}$ is obtained from relation (3.6) $\frac{\partial y}{\partial t}(t,\bar{x}) = -q(u(t,\bar{x}))$. In particular, if $\bar{x}$ is chosen positive then $u(t,\bar{x}) = u_+$ since the shock is moving to the left. Hence

$$y(t,\bar{x}) = y_0(\bar{x}) - tq(u_+).$$

Together with (3.8) we conclude that the surface is, on the one hand, moving downwards because of removal of material and, on the other hand, the kink is moving to the left (see fig. 3.20).

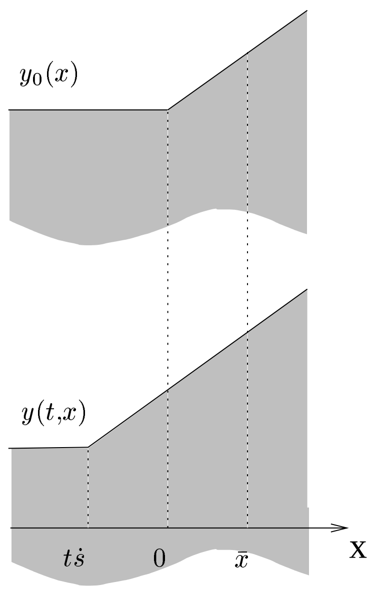

Figure 3.20 Evolution of the material surface with a kink traveling to the left

In our second example, we assume that the jump upward is stronger with $u_+ > u_*$ (see fig. 3.21(a)). Now, a single shock is no longer an entropy solution of the problem because $q(u)$ is located above and below the chord between $q(u_-)$ and $q(u_+)$. However, we can construct a weak piecewise classical solution by combining a shock wave with a rarefaction wave. In order for the shock wave to be entropy consistent, we choose again the right state $\bar{u} \leq u_*$.

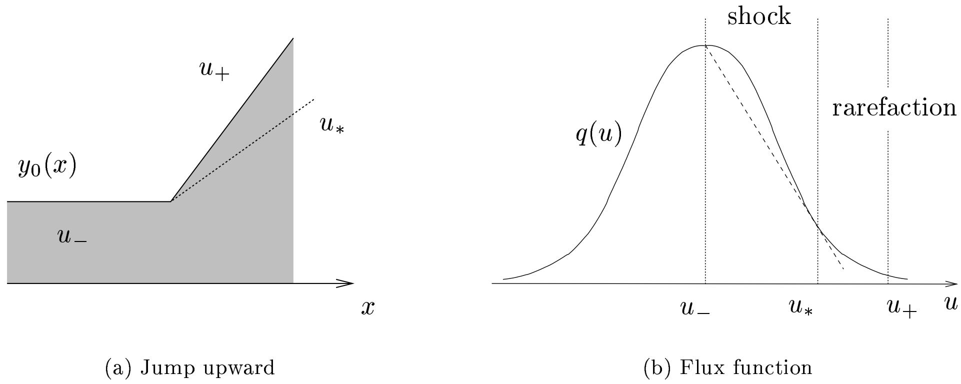

Figure 3.21 Riemann initial value with strong jump for the ion etching equation

Then we try to continue the solution with a rarefaction wave between the values $\bar{u}$ and u_+ which requires q' to be invertible on $[\bar{u},u_+]$. Since the combined solution must be a weak solution, we have the requirement that the right value $(q')^{-1}(\dot{s})$ generated by the rarefaction wave at the shock location $x/t = \dot{s}$ is equal to $\bar{u}$ since otherwise the shock speed $\dot{s} = (q(\bar{u}) - q(u_-))/(\bar{u} - u_-)$ is not correct. This leads to the requirement that $(q(\bar{u}) - q(u_-))/(\bar{u} - u_-) = q'(\bar{u})$, i.e. the chord between $q(u_-)$ and $q(\bar{u})$ must be tangent to the flux function in $\bar{u}$. The only point which satisfies this requirement is actually u_* giving rise to the entropy solution shown in fig. 3.22(a).

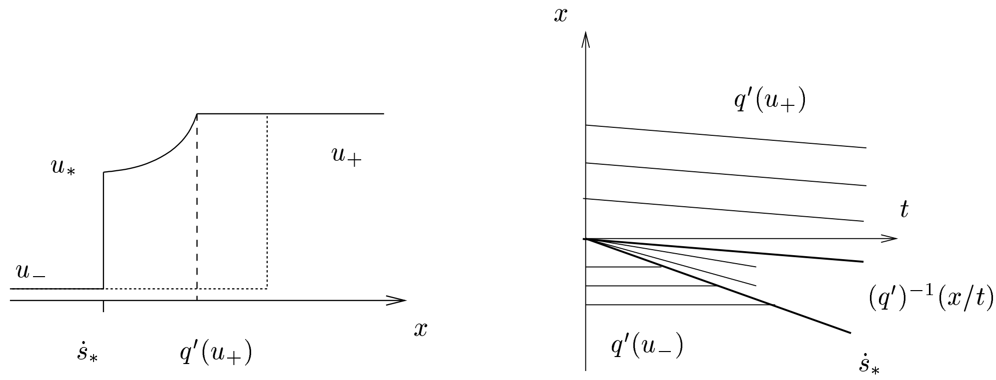

(a) Solution (b) Characteristics

Figure 3.22 Entropy solution for the initial value in fig. 3.21(a)

For a downward jump the situation is reversed: if $u_- = 0$ and $u_+ > -u_*$, the solution simply consists of a rarefaction wave (fig. 3.23(a)) and if $u_+ < -u_*$ it is a combination of a shock and a rarefaction wave (fig. 3.23(b)).

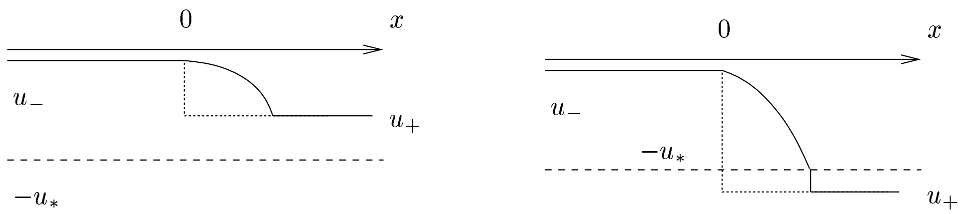

(a) Weak downward jump (b) Strong downward jump

Figure 3.23 Entropy solutions for initial values with downward jump in the slopes

Finally, for a more complicated material with a flux having several extrema, situations like the one depicted in fig. 3.24 can appear. For the configuration of the initial surface shown in fig. 3.25(a), the entropy solution now consists of a jump, followed by a (very small) rarefaction wave which is again followed by a stationary jump and then, symmetrically, again a small rarefaction wave and a final jump to u_+ (see fig. 3.25(b)).

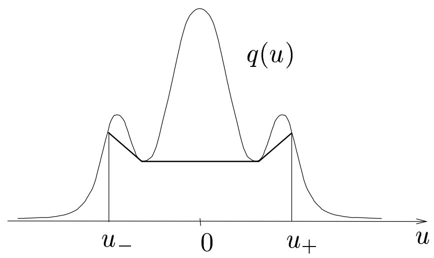

Figure 3.24 Flux function modeling a more complicated material behavior

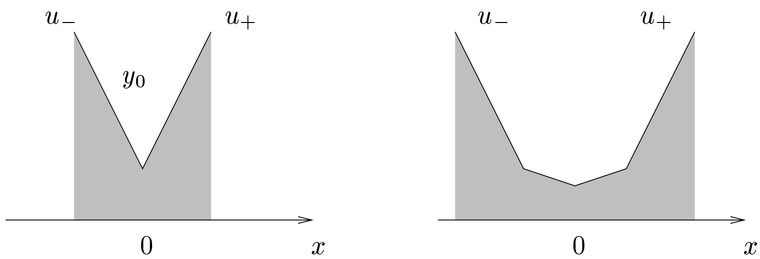

(a) Initial configuration (b) Solution

Figure 3.25 Entropy solution in the case of complicated material behavior

For further details concerning the ion beam etching (also in the case of compound materials which leads to free boundary value problems), we refer to [4].

4 Systems of conservation laws

4.1 Characteristic surfaces

We begin with some general comments on non-linear systems of balance laws for the variables $\boldsymbol{U} = (U_1, \ldots, U_m) \in \mathcal{S} \subset \mathbb{R}^m$. Starting in the form

$$\operatorname{div}_{\boldsymbol{y}} \mathcal{A}_k(\boldsymbol{U}) = Q_k(\boldsymbol{U}), \quad k = 1, \ldots, m \tag{4.1}$$

with generalized fluxes $\mathcal{A}_k = (\mathcal{A}_k^{(1)}, \ldots, \mathcal{A}_k^{(N)}) \in C^1(\mathcal{S}, \mathbb{R}^N)$, we rewrite the problem in quasi-linear form

$$\sum_{j=1}^{m} (\boldsymbol{a}_{kj}(\boldsymbol{U}) \cdot \nabla) U_j = Q_k, \quad k = 1, \ldots, m \tag{4.2}$$

where the vectors $\boldsymbol{a}_{kj} = (a_{kj}^{(1)}, \ldots, a_{kj}^{(N)})$ are defined by $a_{kj}^{(i)} = \frac{\partial \mathcal{A}_k^{(i)}}{\partial U_j}$. We recall that the system is hyperbolic if the matrix $A(\boldsymbol{\xi}, \boldsymbol{U}) = (\boldsymbol{\xi} \cdot \boldsymbol{a}_{kj}(\boldsymbol{U}))$ has only real eigenvalues for all $\boldsymbol{\xi} \in \mathbb{R}^N$ and all $\boldsymbol{U} \in \mathcal{S}$. Let us now consider (4.2) together with boundary conditions on a hypersurface $\Gamma \subset \mathbb{R}^N$. If we want to determine $\boldsymbol{U}(\boldsymbol{y})$ at some point $\boldsymbol{y} \notin \Gamma$ starting from known values $\boldsymbol{\phi} \in \Gamma$, we need information about the rate of change of $\boldsymbol{U}$ in a direction normal to Γ . This information should be provided by the system (4.2) which, in fact, consists of linear combinations of directional derivatives $\boldsymbol{a}_{kj} \cdot \nabla$. In particular, we can hope to get information about the rate of change of $\boldsymbol{U}$ in normal direction if the directions $\boldsymbol{a}_{kj}$ have suitable normal components. Splitting the derivative according to

$$\boldsymbol{a}_{kj} \cdot \nabla = (\boldsymbol{n} \cdot \boldsymbol{a}_{kj})(\boldsymbol{n} \cdot \nabla) + (\boldsymbol{a}_{kj} - (\boldsymbol{n} \cdot \boldsymbol{a}_{kj})\boldsymbol{n}) \cdot \nabla$$

in a normal and a tangential derivative and combining the source term with the tangential derivative along Γ

$$b_k(\boldsymbol{U}|_\Gamma) = Q_k(\boldsymbol{U}|_\Gamma) - \sum_{j=1}^{m} (\boldsymbol{a}_{kj} - (\boldsymbol{n} \cdot \boldsymbol{a}_{kj})\boldsymbol{n}) \cdot \nabla\, U_j|_\Gamma \,,$$

we reformulate (4.2) on Γ as

$$A(\boldsymbol{n}, \boldsymbol{U}|_\Gamma)(\boldsymbol{n} \cdot \nabla)\boldsymbol{U} = \boldsymbol{b}(\boldsymbol{U}|_\Gamma) \tag{4.3}$$

where $A_{kj}(\boldsymbol{\xi}, \boldsymbol{U}) = (\boldsymbol{\xi} \cdot \boldsymbol{a}_{kj}(\boldsymbol{U}))$. Prescribing $\boldsymbol{U}|_\Gamma = \boldsymbol{\phi}$, we see that all normal derivatives $(\boldsymbol{n} \cdot \nabla)\boldsymbol{U}$ are obtained form the partial differential equation provided $A(\boldsymbol{n}, \boldsymbol{\phi})$ is invertible. We therefore distinguish two cases:

1) If $\det A(\boldsymbol{n}(\boldsymbol{y}), \boldsymbol{\phi}(\boldsymbol{y})) \neq 0$ for all $\boldsymbol{y} \in \Gamma$ (i.e. Γ is *nowhere-characteristic*), the differential equation provides all normal derivatives

$$(\boldsymbol{n} \cdot \nabla)\boldsymbol{U} = A^{-1}(\boldsymbol{n}, \boldsymbol{\phi})\boldsymbol{b}(\boldsymbol{\phi})$$

so that $\boldsymbol{U}$ is determined in a neighborhood of Γ by the given values $\boldsymbol{\phi}$ and the partial differential equation. Hence, nowhere-characteristic surfaces are suitable for prescribing arbitrary data $\boldsymbol{\phi}$.

2) The situation is very much different in points $\boldsymbol{y} \in \Gamma$ where Γ is *characteristic*, i.e. $\det A(\boldsymbol{n}(\boldsymbol{y}),\boldsymbol{\phi}(\boldsymbol{y})) = 0$. In this case the system (4.3) yields compatibility conditions on the data $\boldsymbol{\phi}$. In fact, let $0 \neq \boldsymbol{r}$ be orthogonal to the image of the matrix $A(\boldsymbol{n}(\boldsymbol{y}),\boldsymbol{\phi}(\boldsymbol{y}))$. Then,

$$0 = \boldsymbol{r} \cdot A(\boldsymbol{n}(\boldsymbol{y}),\boldsymbol{\phi}(\boldsymbol{y}))(\boldsymbol{n} \cdot \nabla)\boldsymbol{U} = \boldsymbol{r} \cdot \boldsymbol{b}(\boldsymbol{\phi}),$$

giving rise to the condition $\boldsymbol{r} \cdot \boldsymbol{b}(\boldsymbol{\phi}) = 0$ which puts restrictions on $\boldsymbol{\phi}$. Consequently, a surface Γ having characteristic points is not suited for prescribing general data $\boldsymbol{\phi}$. However, if all points of Γ are characteristic (i.e. if Γ is a characteristic surface), we have additional knowledge about the behavior of the solution along Γ . Exactly this property has been used in the method of characteristics where $\boldsymbol{y}$ was a two-dimensional variable and the hypersurface Γ is one-dimensional (called characteristic ground curve). In this case, b is just the derivative along Γ if there are no sources $Q = 0$, so that $\boldsymbol{r} \cdot \boldsymbol{b}(\boldsymbol{\phi}) = 0$ implies that the solution must be constant along characteristic ground curves.

4.2 The Saint-Venant system

As example for a hyperbolic system, we will now consider the Saint-Venant (or shallow water) equations. These equations have a wide range of applications, for example in the prediction of water levels along rivers. A good prediction of the water height is necessary to load ships maximally under the constraint that they can reach their destination without the problem of ground contacts.

Figure 4.1 For optimal loading of ships, a prediction of the water height along the river is mandatory

The shallow water system is also used in the prediction of pollutant transport in rivers and for estimating the effects of breaking dams.

Considering, for example, the river Rhine we find typical dimensions

extension	typical size
length	1000 km
width	100 m
depth	5 m

which indicates that a one-dimensional model should be adequate, mapping a river segment of length L to the interval $[0,L]$. Then, the Saint-Venant equations are derived by a balancing consideration for water mass and momentum (for details and references we refer to [9]). Assuming constant density, the water mass contained in a slice of width dx at position x is $dm = \rho F(t,x)dx$ where F is the river cross section at position x and time t (see fig. 4.2).

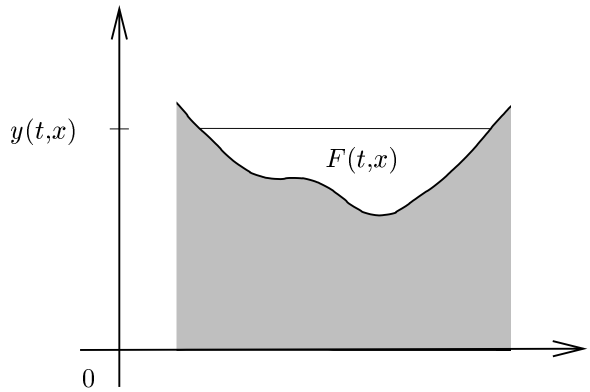

Figure 4.2 River cross section at position $x \in [0,L]$

Similarly, the mass flux is given by $\rho D(t,x)dt$ where $D = vF$ and $v(t,x)$ is an averaged flow velocity at position x. Taking into account sources d caused by influx from the sides, we obtain

$$\frac{\partial F}{\partial t} + \frac{\partial D}{\partial x} = d$$

The momentum balance leads to an equation of the form

$$\frac{\partial D}{\partial t} + \frac{\partial}{\partial x}(vD) = -gF\left(\frac{\partial y}{\partial x} + S_f\right) + v'd$$

where g is the gravitational constant and y is the water height over sea level which is related to F by some (measured) function $y = H(x,F)$. The term S_f is an empirical friction model taking into account momentum loss due to bottom friction. A typical form is $S_f = \alpha|v|v/R^{4/3}$ where $R = F/U$ and U is the wetted perimeter. Finally, v' is the velocity of the lateral inflows in the direction of the main flow. Writing the equations in quasi-linear form, we find

$$\begin{aligned} &\frac{\partial F}{\partial t} + v\frac{\partial F}{\partial x} + F\frac{\partial v}{\partial x} = d \\ &\frac{\partial v}{\partial t} + v\frac{\partial v}{\partial x} + g\frac{\partial H}{\partial F}\frac{\partial F}{\partial x} = -gF\left(\frac{\partial H}{\partial x} + S_f\right) + (v' - v)d \end{aligned} \tag{4.4}$$

To investigate the hyperbolicity, we set up the matrix A

$$A(\boldsymbol{\xi},F,v) = \begin{pmatrix} \xi_1 + \xi_2 v & \xi_2 F \\ \xi_2 g \frac{\partial H}{\partial F} & \xi_1 + \xi_2 v \end{pmatrix}$$

which has eigenvalues $\lambda_{1/2} = \xi_1 + \xi_2 v \mp \sqrt{\xi_2^2 F g \frac{\partial H}{\partial F}}$. Obviously, the eigenvalues are real because at a fixed position x , larger cross section F implies a larger water height $H(x,F)$ giving rise to a positive derivative $\frac{\partial H}{\partial F} > 0$. Hence, the Saint-Venant equations are of hyperbolic type. Considering (4.4) on the domain $\Omega = \mathbb{R}^+ \times (0,L)$ we have to prescribe boundary values. For the surface $\Gamma_0 = \{0\} \times (0,L)$ we find the normal vector $\boldsymbol{n} = (-1,0)$ so that

$$A(\boldsymbol{n},F,v) = \begin{pmatrix} -1 & 0 \\ 0 & -1 \end{pmatrix}$$

always a nonzero determinant. Consequently, Γ_0 is nowhere-characteristic and arbitrary initial data can be prescribed. Conversely, let us now determine the characteristic surfaces Γ for which $\det A(\boldsymbol{n},F,v) = 0$. Using the parameterization

$$\Gamma = \{(t,\gamma(t)) : t > 0\}$$

we obtain with $\boldsymbol{n} = \alpha(\dot\gamma(t), -1)$, $\alpha = (1 + \dot\gamma^2)^{-1/2}$ the condition

$$0 = \det \begin{pmatrix} \dot\gamma - v & -F \\ -g\frac{\partial H}{\partial F} & \dot\gamma - v \end{pmatrix} = \det(\dot\gamma \mathrm{id} - A((0,1),F,v))$$

which is satisfied if and only if $\dot\gamma$ is an eigenvalue of $A((0,1),F,v)$. Hence, there exist two families of characteristic curves (see fig. 4.3) which are defined by

$$\dot\gamma = \lambda_1(\gamma) \qquad \lambda_1 = v - \sqrt{Fg\frac{\partial H}{\partial F}}$$

$$\dot\gamma = \lambda_2(\gamma) \qquad \lambda_2 = v + \sqrt{Fg\frac{\partial H}{\partial F}}$$

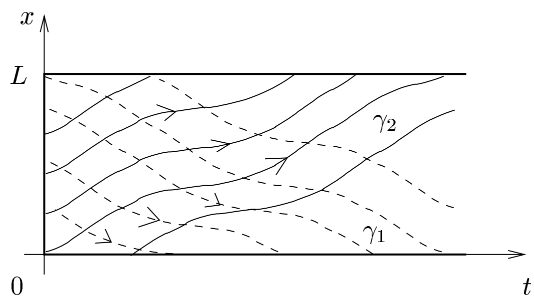

Figure 4.3 Two families of characteristic curves for the shallow water system

The orientation of the two families of curves at the boundaries $\mathbb{R}^+ \times \{0\}$ and $\mathbb{R}^+ \times \{L\}$ are important to determine the number of boundary conditions which have to be supplied. In the case $|v| < \sqrt{Fg\frac{\partial H}{\partial F}}$ (subcritical flow) one has to prescribe one condition at each boundary (for example the water level at the upper and lower end of the observed river segment). The supercritical case $|v| > \sqrt{Fg\frac{\partial H}{\partial F}}$ is characterized by the fact that two boundary conditions (level and flux) have to be prescribed at one and no boundary condition at the other boundary (see fig. 4.4).

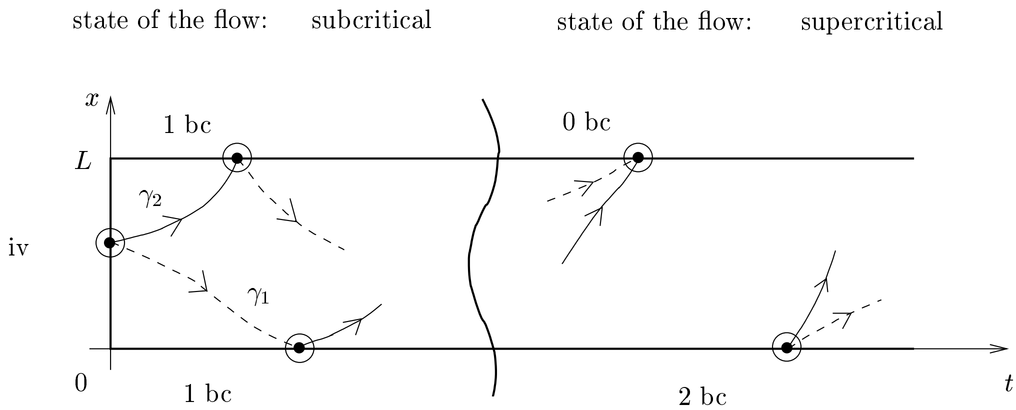

Figure 4.4 Number of boundary conditions (bc) for sub- and supercritical flow

In the following we are going to consider the Riemann problem for a simplified version of the shallow water system. First, we assume that the river has no slope and always a rectangular cross section. As variable for the height we introduce $h(t,x)$ so that $F(t,x) = bh(t,x)$ (see fig. 4.5).

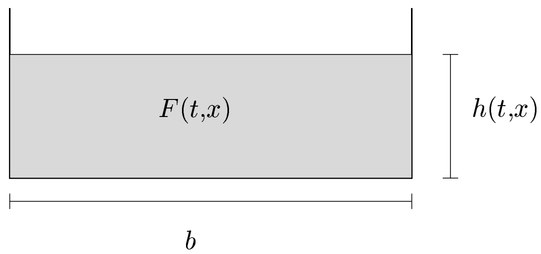

Figure 4.5 River geometry for the model problem

Moreover, we assume that there are no lateral in- and outflows and no friction. By choosing the length scale L, velocity scale $V = \sqrt{gL}$ and time scale $T = L/V$, we eventually get the system (in scaled variables)

$$\frac{\partial h}{\partial t} + \frac{\partial hv}{\partial x} = 0, \qquad \frac{\partial hv}{\partial t} + \frac{\partial}{\partial x}(hv^2 + h^2/2) = 0, \tag{4.5}$$

or with $q = hv$, $\boldsymbol{u} = (h,q)$ and $\boldsymbol{G}(\boldsymbol{U}) = (q,q^2/h + h^2/2)$ and Riemann initial data

$$\frac{\partial \boldsymbol{U}}{\partial t} + \frac{\partial}{\partial x}\boldsymbol{G}(\boldsymbol{U}) = 0, \qquad \boldsymbol{U}(0,x) = \begin{cases} \boldsymbol{U}_- & x < 0 \\ \boldsymbol{U}_+ & x > 0 \end{cases} \tag{4.6}$$

Typical Riemann initial conditions are shown in fig. 4.6.

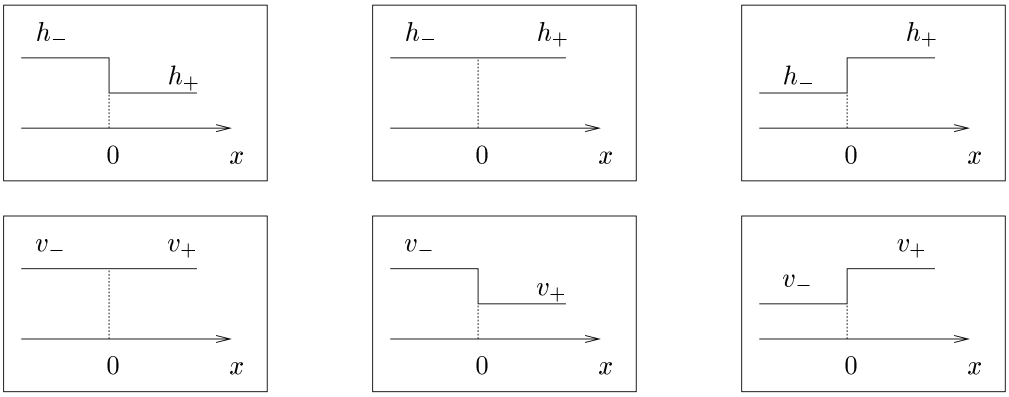

Figure 4.6 Possible Riemann initial values for water height and velocity

4.3 Rarefaction waves

We start with the construction of specific solutions of the system (4.5) called k-simple waves with $k = 1{,}2$. If $\boldsymbol{r}_k(\boldsymbol{U})$ is an eigenvector of $\nabla \boldsymbol{G}(\boldsymbol{U})$ with corresponding eigenvalue $\lambda_k(\boldsymbol{U})$, we proceed as follows:

1) we first solve $\boldsymbol{\gamma}'(s) = \boldsymbol{r}_k(\gamma(s))$ with some initial condition
2) we then solve $\frac{\partial w}{\partial t} + \lambda_k(\gamma(w))\frac{\partial w}{\partial x} = 0$ with initial conditions
3) finally, we set $\boldsymbol{U}(t,x) = \boldsymbol{\gamma}(w(t,x))$

The function $\boldsymbol{U}$ (the k-simple wave) is a solution of (4.5) because

$$\frac{\partial \boldsymbol{U}}{\partial t} = \boldsymbol{\gamma}'\frac{\partial w}{\partial t} = -\boldsymbol{r}_k\lambda_k\frac{\partial w}{\partial x} == -\nabla \boldsymbol{G}\,\boldsymbol{r}_k\frac{\partial w}{\partial x} = -\nabla \boldsymbol{G}\,\frac{\partial \boldsymbol{U}}{\partial x} = -\frac{\partial}{\partial x}\boldsymbol{G}(\boldsymbol{U}).$$

In order to work out this program with rarefaction solutions w, we first determine the curves $\boldsymbol{\gamma}$. Eigenvalues and eigenvectors of $\nabla \boldsymbol{G}$ are given by

$$\lambda_{1/2} = v \mp \sqrt{h} = \frac{q}{h} \mp \sqrt{h}, \qquad \boldsymbol{r}_{1/2} = (1,\lambda_{1/2})$$

and the curves in (h,q) space are (see fig. 4.7)

$$\boldsymbol{\gamma}^{(1/2)}(h) = (h,\bar{\kappa}_{1/2}h \mp 2h^{3/2}), \qquad \bar{\kappa}_{1/2} = \bar{v} \pm 2\sqrt{\bar{h}}$$

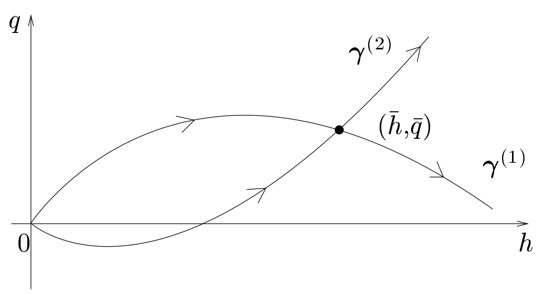

Figure 4.7 Integral curves of eigenvectors fields $\boldsymbol{r}_1$ and $\boldsymbol{r}_2$

In the second step, we solve the scalar equation for w which turns into a conservation law by introducing the flux function

$$g_k(w) = \int_0^w \lambda_k(\boldsymbol{\gamma}^{(k)}(\sigma))\,d\sigma, \qquad w > 0.$$

Note that $\lambda_k(\boldsymbol{\gamma}^{(k)}(\sigma)) = \frac{d}{d\sigma}\gamma_2^{(k)}(\sigma)$ and hence $g_k(w) = \gamma_2^{(k)}(w)$ so that g_1 is concave and g_2 is convex (the graphs of g_1 , g_2 coincide with the curves in fig. 4.7). Consequently, the correct entropy solution of

$$\frac{\partial w}{\partial t} + \frac{\partial}{\partial x} g_k(w) = 0, \quad w(0,x) = \begin{cases} w_- & x < 0 \\ w_+ & x > 0 \end{cases}$$

is a rarefaction wave if $g_k'(w_+) > G_k'(w_-)$ which implies $w_- > w_+$ for $k = 1$ and $w_- < w_+$ in the case $k = 2$. In both cases, the property $g_k'' \neq 0$ together with $g_k' = \lambda_k(\boldsymbol{\gamma}^{(k)})$ implies $\boldsymbol{r}_k \cdot \nabla\lambda_k \neq 0$ (i.e. the pair $(\lambda_k,\boldsymbol{r}_k)$ is *genuinely nonlinear*). As specific example of a w-rarefaction wave, we consider $k = 1$, $\bar{h} = 1$, $\bar{v} = 0$, $w_- = 4$, and $w_+ = 1$. In this case, $\bar{\kappa}_1 = 2$ and $g_1(w) = 2w - 2w^{3/2}$ with derivative $g_1'(w) = 2 - 3\sqrt{w}$. Note that the rarefaction solution is based on

$$(g_1')^{-1}(\xi) = (2 - \xi)^2/9.$$

and has the complete form (see also fig. 4.8)

$$w(t,x) = \begin{cases} w_- = 4 & x/t < g_1'(w_-) = -4 \\ (2 - x/t)^2/9 & -4 < x/t < -1 \\ w_+ = 1 & x/t > g_1'(w_+) = -1 \end{cases}$$

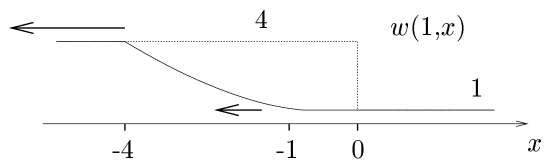

Figure 4.8 Solution of the Riemann problem for the auxiliary quantity w

Based on w , we now define the 1-rarefaction wave $\boldsymbol{U}^0(x) = \boldsymbol{\gamma}^{(1)}(w(0,x))$ (see fig. 4.9(a))

$$h(t,x) = w(t,x), \qquad v(t,x) = 2 - 2\sqrt{w(t,x)}$$

which solves the Riemann problem (4.6) with

$$\boldsymbol{U}^0(x) = \boldsymbol{\gamma}^{(1)}(w(0,x)) = \begin{cases} (4,-8) & x < 0 \\ (1,0) & x > 0 \end{cases}$$

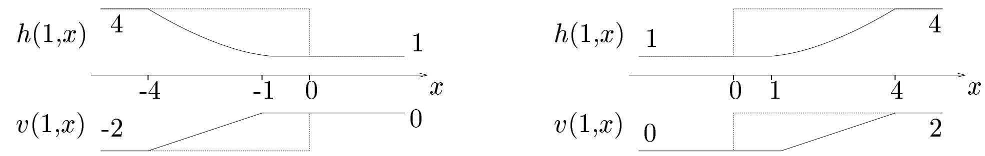

(a) 1-rarefaction (b) 2-rarefaction

Figure 4.9 Rarefaction waves of the shallow water system

Similarly, a 2-rarefaction wave is obtained with $\bar{h} = 1$, $\bar{v} = 0$, $w_- = 1$, $w_+ = 4$, giving rise to $\boldsymbol{U}_- = (1,0)$, and $\boldsymbol{U}_+ = (4,8)$ (see fig. 4.9(b)).

4.4 Shock waves

Similar to the scalar case, one introduces weak solutions for systems of conservation laws: a function $\boldsymbol{U} \in [\mathbb{L}^\infty_{loc}(\mathbb{R}^2)]^2$, $\boldsymbol{U}(t,x) = 0$ for $t < 0$ is called *weak solution* of (4.6) if

$$\mathrm{div}_{\boldsymbol{y}} \mathcal{A}_i(\boldsymbol{U}) = U_i^0 \delta_{\Gamma_0}, \quad \text{in } \mathscr{D}'(\mathbb{R}^2), \quad i = 1,2$$

where $\mathcal{A}_i(\boldsymbol{U}) = (U_i, G_i(\boldsymbol{U}))$, $\boldsymbol{y} = (t,x)$ and $\Gamma_0 = \{0\} \times \mathbb{R}$.

Using the divergence relation (3.3), one shows that a piecewise classical solution is a weak solution if and only if $[\mathcal{A}_i(\boldsymbol{U})] \cdot \boldsymbol{n} = 0$ on the shock curve Γ_s . In terms of the slope $\dot{s}(t)$ of the shock curve, the condition reads

$$\dot{s}[U_i] = [G_i(\boldsymbol{U})], \qquad i = 1,2$$

and for the specific case of the shallow water system

$$\dot{s}[h] = [q], \qquad \dot{s}[q] = [q^2/h + h^2/2].$$

With the first condition one determines the shock speed $\dot{s} = [q]/[h]$ which then yields with the second relation

$$[q]^2 = [h][q^2/h + h^2/2]. \tag{4.7}$$

This relation implies that only selected pairs of states (q,h) and $(\bar{q},\bar{h})$ can be connected by a shock. Inserting $[q] = q - \bar{q}$, $[h] = h - \bar{h}$ and $[q^2/h + h^2/2] = q^2/h + h^2/2 - \bar{q}^2/\bar{h} + \bar{h}^2/2$, we can transform (4.7) into the relation

$$q = \bar{v}h \mp (h - \bar{h})\sqrt{(\frac{1}{h} + \frac{1}{\bar{h}})/2} \tag{4.8}$$

Hence, the states (h,q) which can be connected with $(\bar{q},\bar{h})$ by a shock are located on two curves $q = q^{(1)}(h)$ and $q = q^{(2)}(h)$ depending on the sign $-$ or $+$ in (4.8) respectively (see fig. 4.10. The corresponding shock speeds are

$$\sigma_{1/2}(\boldsymbol{U},\bar{\boldsymbol{U}}) = \bar{v} \mp \sqrt{\frac{h}{2\bar{h}}(h + \bar{h})}.$$

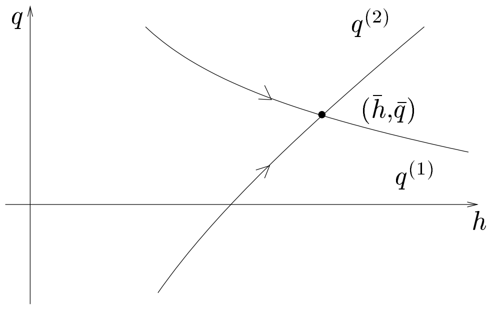

Figure 4.10 States which can be connected with $(\bar{q},\bar{h})$ by a weak solution with shock

In order to check which combination of states not only leads to a weak solution but also satisfies an entropy condition, we set $\boldsymbol{U}_- = (\bar{h},\bar{q})$ and consider successively $\boldsymbol{U}_+$ on the branches formed by the curves $q^{(1)}(h)$ and $q^{(2)}(h)$ in fig. 4.10. First, we consider the case in fig. 4.11(a). A simple calculation shows that on this branch

$$\lambda_1^- = \lambda_1(\boldsymbol{U}_-) < \sigma_1(\boldsymbol{U}_+,\boldsymbol{U}_-) < \lambda_1(\boldsymbol{U}_+) = \lambda_1^+$$

which leads to a configuration of characteristic ground curves as shown in fig. 4.11(b).

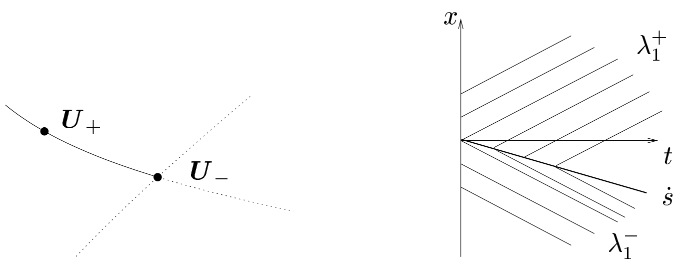

(a) Riemann states (b) Characteristics

Figure 4.11 Situation in which shock solution is not entropy consistent

Obviously, the characteristics do not run into the shock and we discard this branch as being entropy violating. On the branch in fig. 4.12(a), on the other hand, we find

$$\lambda_1^+ < \sigma_1(\boldsymbol{U}_+,\boldsymbol{U}_-) < \min\{\lambda_1^-,\lambda_2^+\}$$

so that λ_1 -characteristic ground curves run into the so called 1-shock (see fig. 4.12(b)).

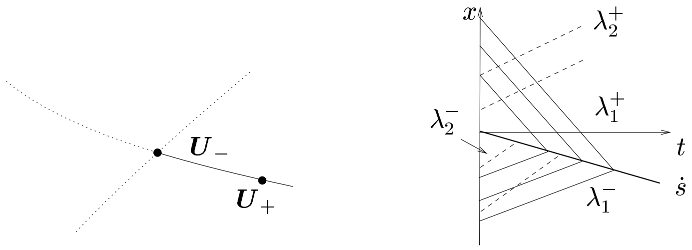

(a) Riemann states (b) Characteristics

Figure 4.12 Situation of an entropy consistent 1-shock

Continuing with the branches of the curve $q^{(2)}$, we find that in the case of fig. 4.13(a)

$$\lambda_2^- < \sigma_2(\boldsymbol{U}_+, \boldsymbol{U}_-) < \lambda_2^+$$

leading to jumps which are not entropy consistent. Finally, a consideration for state $\boldsymbol{U}_+$ on the branch in fig. 4.14(a) shows that

$$\max\{\lambda_1^-, \lambda_2^+\} < \sigma_2(\boldsymbol{U}_+, \boldsymbol{U}_-) < \lambda_2^-$$

so that λ_2-characteristics run into the entropy consistent 2-shock (see fig. 4.14(b)).

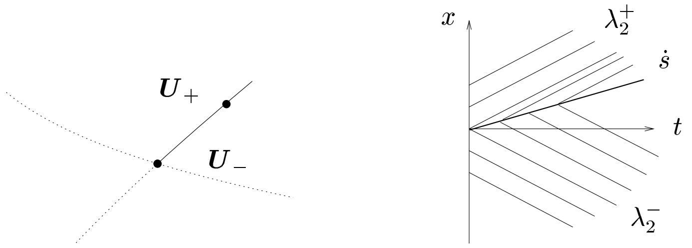

(a) Riemann states (b) Characteristics

Figure 4.13 Situation in which shock solution is not entropy consistent

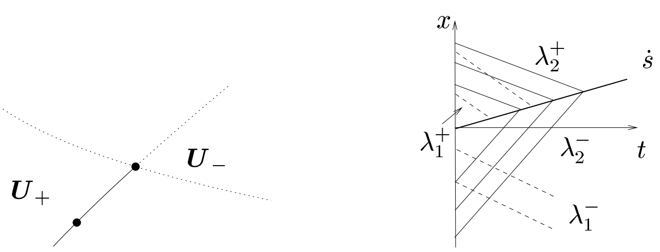

(a) Riemann states (b) Characteristics

Figure 4.14 Situation of an entropy consistent 2-shock

Examples for 1- and 2-shocks are shown in fig. 4.15(a) and fig. 4.15(b) for $\boldsymbol{U}_- = (1{,}0)$ and $\boldsymbol{U}_+ = (2, -\sqrt{3/4})$ respectively $\boldsymbol{U}_+ = (1/2, -\sqrt{3/8})$.

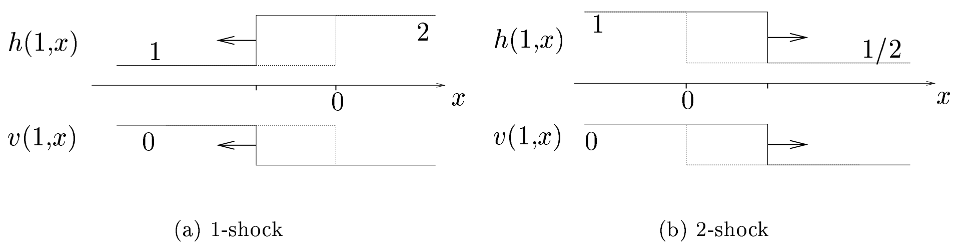

Figure 4.15 Shock solutions for the shallow water system

Summarizing our considerations we conclude that the states $\boldsymbol{U}_+$ which can be connected with the state $\boldsymbol{U}_-$ by a shock wave are located on the lower branches of the $q^{(1)}$ and the $q^{(2)}$ curves which we denote by $S_1(\boldsymbol{U}_-)$ and $S_2(\boldsymbol{U}_-)$ respectively (see fig. 4.16).

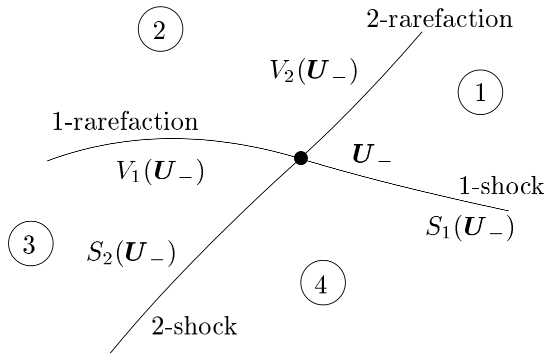

Figure 4.16 In regions 1 – 4 the solution of the Riemann problem is a combination of shocks and rarefaction waves

A connection between $\boldsymbol{U}_+$ and $\boldsymbol{U}_-$ with an entropy consistent rarefaction wave is possible if $\boldsymbol{U}_+$ is located on the upper branches of $\gamma^{(1)}$ or $\gamma^{(2)}$ (see fig. 4.7) which we denote $R_1(\boldsymbol{U}_-)$ and $R_2(\boldsymbol{U}_-)$. If $\boldsymbol{U}_+$ is located on none of the branches S_1,S_2,R_1 , and R_2 , a connection with a single shock or rarefaction is not possible. For example, if $\boldsymbol{U}_+$ is located in region 1 (fig. 4.16), there exists a unique $\boldsymbol{U}_* \in S_1(\boldsymbol{U}_-)$ such that $\boldsymbol{U}_+ \in R_2(\boldsymbol{U}_*)$ (see fig. 4.17).

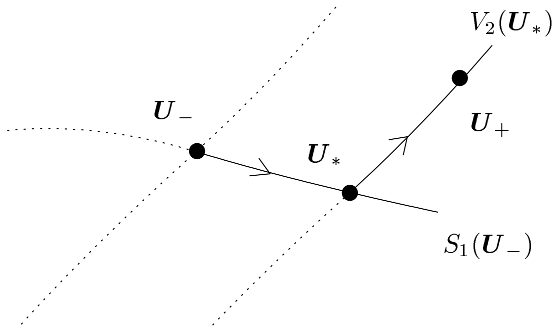

Figure 4.17 Connection of states $\boldsymbol{U}_-$ and $\boldsymbol{U}_+$ via the intermediate state $\boldsymbol{U}_*$

The corresponding (t,x) diagram and the solution at time $t = 1$ which is a combination of a 1-shock and a 2-rarefaction are shown in fig. 4.18.

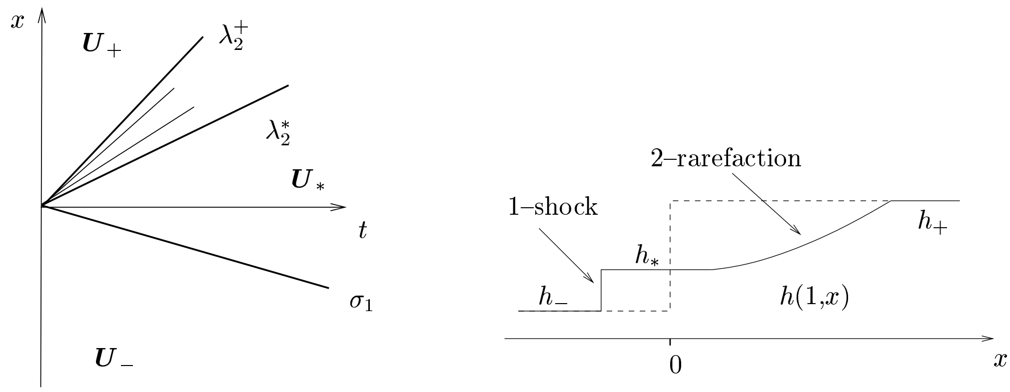

(a) Characteristics (b) Water height

Figure 4.18 Combination of a 1-shock and a 2-rarefaction wave

For $\boldsymbol{U}_+$ in region 2, two rarefaction waves are connected (fig. 4.19), region 3 corresponds to a 1-rarefaction and a 2-shock (fig. 4.20(a)). Finally, for $\boldsymbol{U}_+$ in region 4, the solution is a combination of two shocks according to fig. 4.20(b).

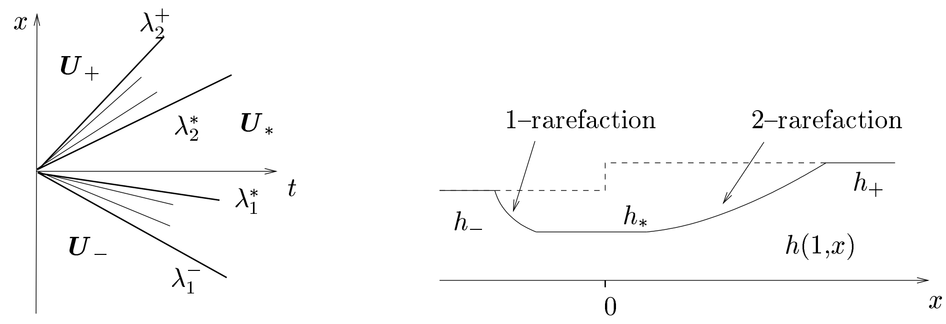

(a) Characteristics (b) Water height

Figure 4.19 Combination of a 1-rarefaction and a 2-rarefaction wave

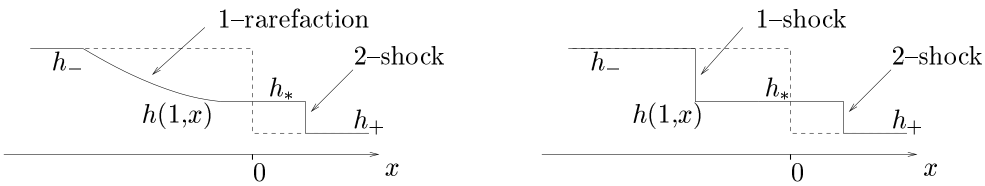

(a) Region 3 (b) Region 4

Figure 4.20 Solutions corresponding to $\boldsymbol{U}_+$ in region 3 and 4 of fig. 4.16

For further details on Riemann problems for non-linear systems of conservation laws in one space dimension we refer, for example, to [7, 10, 6].

Bibliography

[1] C Cercignani. *The Boltzmann Equation and its Applications.* Springer, 1988.

[2] Alexandre J. Chorin and Jerrold E. Marsden. *A Mathematical Introduction to Fluid Mechanics.* Springer, 3rd edition, 1993.

[3] Lawrence C. Evans. *Partial Differential Equations*, volume 9 of *Graduate Studies in Mathematics.* American Mathematical Society, 1998.

[4] Avner Friedman. *Mathematics in Industrial Problems*, volume 16 of *The IMA Volumes in Mathematics and its Applications.* Springer, 1988.

[5] Edwige Godlewski and Pierre-Arnaud Raviart. *Hyperbolic systems of conservation laws.* Mathematiques & Applications. Ellipses, Paris, 1991.

[6] Edwige Godlewski and Pierre-Arnaud Raviart. *Numerical approximation of hyperbolic systems of conservation laws*, volume 118 of *Applied Mathematical Sciences.* Springer, New York, 1996.

[7] J. Kevorkian. *Partial differential equations. Analytical solution techniques.* Mathematics Series. Wadsworth & Brooks/Cole, Pacific Grove, Ca, 1990.

[8] J. Necas, J. Malek, M. Rokyta, and M. Ruzicka. *Weak and measure-valued solutions to evolutionary PDEs.*, volume 13 of *Applied Mathematics and Mathematical Computation.* Chapman & Hall, London, 1996.

[9] Peter Rentrop and Gerd Steinebach. Model and numerical techniques for the alarm system of river rhine. *Surv. Math. Ind.*, 6(4):245–265, 1997.

[10] Joel Smoller. *Shock waves and reaction-diffusion equations*, volume 258 of *Grundlehren der Mathematischen Wissenschaften.* Springer, New York, 2nd edition, 1994.

[11] Matthew Witten. *Hyperbolic partial differential equations : populations, reactors, tides and waves, theory and applications.* Pergamon Press, Oxford, 1983.